AMBER, I. and O'DONOVAN, T.S. 2018. Natural convection induced by the absorption of solar radiation: a review. *Renewable and sustainable energy reviews* [online], 82(Part 3), pages 3526-3545. Available from: https://doi.org/10.1016/j.rser.2017.10.106

Natural convection induced by the absorption of solar radiation: a review.

AMBER, I. and O'DONOVAN, T.S.

2018

Natural convection induced by the absorption of solar radiation: A review.

I.Amber[1] and T.S.O'Donovan[2]

Institute of Mechanical Process and Energy, Engineering
Heriot-Watt University, Edinburgh,
EH14 4AS, United Kingdom
Email: ityonamber@gmail.com

Abstract

Natural convection primarily driven by the absorption of thermal energy known as penetrative or thermo-convection is a topic that generates attention due to its importance in various physical systems. A very common example of where this process can be found in geophysical systems such as lakes, where radiation induced natural convective transport have been seen to influence water temperature, biological activity and water quality.
The present paper reviews previous analytical, experimental and numerical studies reported in literature concerning natural convection driven by absorption of thermal radiation. Many of the reviewed studies were motivated by the interest of investigators to understand the physical processes in volumetric absorption thermal radiation in a fluid layer process and its associated energy transport.
In this class of problems, temperature fields are generally described as non-linear and the associated fluid flow is considered rather complex owing to coupling between the direct absorption of radiation and fluid flow. Parametric investigations for the effect of various parameters of interest such as the Rayleigh numbers, Prandtl numbers, spectral nature of incident radiative flux, optical depth, fluid absorptivity, aspect ratio, albedo and boundary emissivity on natural convection have been investigated.
The overall aim of the current review is to present a comprehensive review of the previous and recent approaches applied in the investigations of radiation induced natural convection in reservoirs. The paper also aims to contribute to improving the understanding of the physical processes, heat transfer and fluid dynamics associated with the thermal energy deposition into a fluid

layer. The paper is also highlight the potential application of this concept to help keep solar energy capture costs to a minimum and inform efficient designs of energy systems based on the concept of direct absorption of thermal energy inside a fluid layer.

Keywords: Natural convection, Radiation, Absorption, Experiment, Scaling, Simulation, analytical.

---

1. Introduction

Natural convection primarily driven force by the direct absorption of thermal energy also known as penetrative or thermo-convection is a subject of great interest to researchers. The energy transfer has been proven to have significant influence on fluid temperatures, biological activity, water quality and mixing of pollutants and sediments [1]. The most common example of this phenomenon is in physical systems such as the Earth's mantle, atmosphere, oceans and lakes [2, 3].
In recent years, this type of natural convection has attracted rapt attention in solar energy applications owing to the method of energy transfer which if efficiently exploited offers benefits such as prediction of water quality, and keeping solar energy capture costs to a minimum.
Critical to efficient thermo-fluid system designs based on the concept of volumetric absorption of solar radiation within a fluid layer is an accurate knowledge of the amount of solar energy absorbed by a fluid layer and different depths and an understanding the mechanisms of the associated physical processes [4].
Analytical [5], experimental [6], numerical [7–9] and scaling [9, 10] investigations on the direct absorption of thermal energy in a fluid layer and the induced thermal convective transport have been performed by different researchers under various contexts and boundary conditions.
Most investigations have been motivated by the quest to understand the process mechanisms and predict the temperature and fluid flow and their dependence on selected control parameters.
Absorption of solar radiation inside a fluid layer is selective and is dependent on the solar spectrum [11]. The absorption of solar radiation penetrating a fluid layer at different depths is generally explained by Beer Lambert law $I = I_0 e^{-\alpha y}$. The law describes the exponential decay of light penetrating a fluid layer at a rate dependent on the intensity, wavelength of light and the

attenuation coefficient of the fluid.

Theoretically, in direct absorption of solar radiation inside a fluid, longer (red) radiation is absorbed within a few metres of penetration inside a fluid layer and as such generates a stabilising effect and a stable stratification. The shorter (blue) wavelengths mostly transmitted, if a fluid layer depth is shallow, the non absorbed solar radiation reaching the bottom surface absorbed and re-emitted, develops a destabilising force which subsequently drives a natural convection in that region.

While a considerable number of works concerning radiation induced natural convection due to absorption of thermal energy has been conducted, at the time of writing this paper, to the best of the authors knowledge, none of the existing literature has conducted nor reported a comprehensive review of subject of radiation-induced natural convection due to solar radiative heating. A number of review articles involving application of nanoparticles to enhance solar energy absorption inside a working fluid have been published over the past decade. Most of these publications have concerned with the experimental and theoretical studies on optical properties and application of nanofluids in direct absorption solar collectors [12]. The successful application of nano-fluids in harvesting solar radiation by direct deposition is dependent on the knowledge of their ability to absorb light energy of the solar spectrum must be known. However, this topic is not within the scope of the present paper.

The aim of this paper is to present a comprehensive review of investigations performed on radiation induced natural convection in reservoirs to provide a better understanding of the thermo-fluid transport process and the possibility of utilising this concept to lower the cost of solar energy systems and enhance system efficiency. Short comings and challenges associated with the various investigation are also reported.

2. Experimental studies for natural convection induced by volumetric absorption of solar radiation

Penetrative convection in a cylindrical test cell was experimentally studied in Walden and Ahlers [13]. The experiments were concerned with the measurements of the Rayleigh numbers and Nusselt numbers used to investigate penetrative convection in fluid layer. The departures of a non-OB (Oberbeck and Boussinesq) system from a conventional OB approximation as well as the nature and sizes of hysteris loops were also investigated in this paper.

Detailed description of the experimental apparatus and procedures are given else where [14] and only briefly described here for brevity. The experiment was carried out in a Helium filled cylindrical test cell of height to diameter (H/D)= 4.72, quasi-statically heated at the bottom surface and the top (upper) surface maintained at a constant temperature. The top and bottom boundaries were made from copper, while side walls were made from stainless steel.

Temperatures were set to a value T_0 which coincides with the maximum fluid density. The top fluid temperature was adjusted to attain a value about just greater that T_0. The expansion coefficient which is kept positive and its value is then varied over a fluid layer height. The temperature dependence of the expansion coefficient was measured and then used to investigate the sources of departures form the OB approximation from a non OB approximation .

A plot of the measured temperature taken at the mid plane of the test cell revealed a constant top temperature that monotonically increased with increased heating. At the lower surface the existence of penetrative convection was found to influence the development of a non-uniform temperature profile.

A plot of the mean fluid density measured across a vertical profile demonstrated a convective instability evident by deep penetration of the convective flow into a locally stable layer for a temperature range between T_0 and T', where T_0 is the temperature at maximum fluid density and T' is an intermediate temperature for which a higher fluid density is attained than at the temperature at the bottom surface.

The effect of control parameters; penetrative parameter ($\mathcal{P}$), Rayleigh (Ra) and Nusselt (Nu) number defined in terms of an effective thermal conductivity on penetrative convective flow was investigated.

An effective thermal conductivity was determined by imposing a time independent heat current (q) and measuring the temperature increase of the bottom while holding constant the temperature of the top plate.

The study identified time-dependent flow states which were generally non periodic with characteristic mean frequencies. In a Boussinesq approximation case, a non-periodic time-dependent behaviour became evident close Ra_c /2 while for a non-Boussinesq approximation and penetrative convection a time-dependent flow is occurred much closer to R_c.

When departure from buoyancy-driven convection was initiated, two dimensional roll patterns were found at a critical Rayleigh number Ra_c for a Boussinesq approximation. For non-Boussinesq conditions over a finite range of Rayleigh numbers near the onset of convection the flow pattern consisted of hexagonal cells.

Penetrative convection phenomena observed were explained based on three stages:

i. For $\mathcal{P} > 1$, the Nusselt number for the onset of time-dependent flow dropped sharply until the flow became time-dependent at the start of natural convection. For greater penetration a region of relative stability exists where the absence or presence of time dependence is influenced by the proximity of the system to a bifurcation between stable states [13];

ii. For $\mathcal{P} > 2$, a series of stable states closely spaced in Nusselt number was observed near Ra_c. Transition between states consists of three dimensional cells which are added or removed from the fluid volume to optimise convective transport at lateral boundaries. The spacing between identified states decreased with increasing $\mathcal{P}$;

iii. For $\mathcal{P} \leqslant 3$, the amplitude of hysteris at Ra_c grew as $\mathcal{P}$ increased toward 2 and then declined at larger values of $\mathcal{P}$.

Webb and Viskanta [15] reported laboratory experiments for the radiation-induced natural convection occurring in a volumetrically heated test cell. The study aimed to describe the interaction of heat transfer and natural convective fluid flow within a vertical fluid layer directly absorbing incident thermal energy incident from a horizontal direction.

Fig 1a shows a schematic of the experimental test apparatus and the incident solar radiation. The experimental test cell with dimensions $48 \times 145 \times 41$mm contained degassified water illuminated by a Quartz halogen lamp with parabolic dichroic (Philips 13117) mirrors through an optically transparent front vertical wall. The test cell external vertical side walls were insulated with 5cm Styrofoam insulation. The top of the test cell was left open for filling. The inner compartment was made from a black 12.7mm thick copper block wall. After about eight to ten hours when the system reached steady state, fluid temperatures were measured while florescent dye injection technique was used to visualise fluid flow field.

Interferograms for a radiation flux incident on the water layer were recorded throughout experiments using a Mach-Zehnder interferometer. Interferograms recorded for incident flux corresponding to $1300\mathrm{W/m}^2$ for aspect ratios 1 and 2 is presented in Fig 1b and Fig 1c for aspect ratio 1 and 2. The difference in fringe densities seen at the respective vertical walls as shown in

Fig 1b and Fig 1c is indicative of absorption of radiation and induced natural induced convective heat transfer. Interpretation of the lines of constant intensity converted to isotherms found each fringe to approximately correspond to a temperature difference of 0.14_oC. Incident radiation deposited correctly into fluid layers of high optical depth was completely attenuated before reaching the opaque walls.

Authors also used the interferograms to also analyse fluid flow patterns. Fluid flow induced by absorptive thermal radiation heating close to the transmitted surface rose to the top of the cavity. Fluid travelled along the top free surface and then into the a thin boundary layer that formed at the opaque wall. The flow observed from the interferograms was later confirmed by flow visualisation experiments. The flow structure found in this case is seen to be different from flows in cavities with differentially heated walls. Experimental results showed the central interior core to be stagnant and stratified. The flow structure lost a centrosymmetry characteristic of natural convection flows in cavities with differentially heated walls. The eddy centre was displaced to a position closer to the cooled side wall due to the direct heating of the core of the flow by solar radiation. [15].

Coates and Patterson [16] experimentally studied the unsteady natural convection in a rectangular tank directly absorbing thermal radiation. Experiments overall objective was to performed a series of laboratory experiments and used to test, verify and validate previous scaling and numerical experiments reported in previous studies.

In fig 2 is a schematic of the test cell used in the experiment. Experimental tank was a box made from Perspex with side walls 20mm thick and a 10mm thickness for walls elsewhere. The Perspex box was placed inside a constant temperature bath filled with filtered water to maintain the tank at constant temperature. The internal compartment consisted of three chambers of different sizes: a large tank of volume of 0.036m^3, a small chamber of volume 0.0054m^3 and the last tank situated below the large and small tanks has a volume 0.018m^3 as shown in fig 2. The bottom tank's sole purpose was to control overheating at the lower boundary.

Perspex lids placed on the top of the tank was placed on spacers to formed a 4cm air gap and a lower lid placed directly on the water water surface to form a non slip boundary. Deionised water inside the test cell was directly irradiated by a 1000W quartz globe spot theatre lamp for maximum, intermediate and low intensities during the experiment [16].

Fluid temperatures and velocities were recorded using thermistors and pattern-

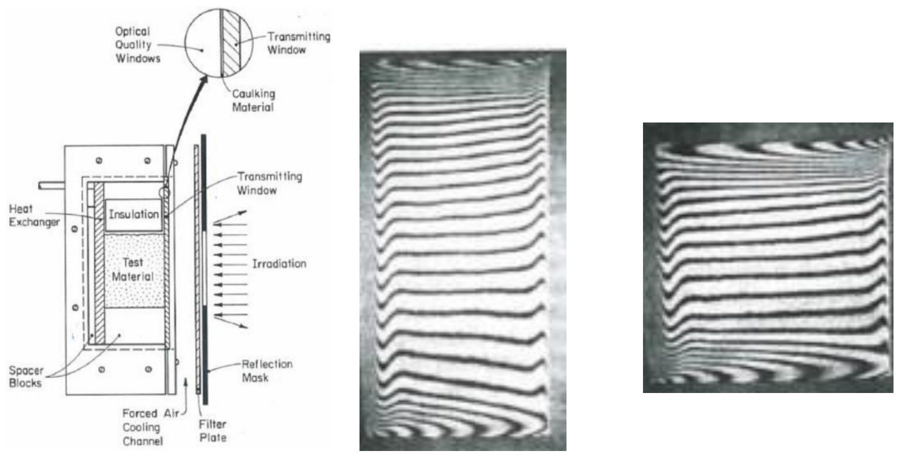

(a) (b) (c)

Figure 1: Experimental set up and results: (a) Test cell (b) Inferrograms for H/W=2 (Left) (c) Inferrograms for H/W=1 [15].

particles (Pliolite) tracer tracking technique.

Fig 3a shows a plot of experimental results for the measured temperature/depth data for three light intensities.Generally the results showed a decrease in fluid temperature with decreasing intensity. From the figure a non uniform temperature profile at all three intensities can easily be seen where temperatures are higher at lower fluid depths and dropped of to much lower values at great fluid depths .

In Fig 3b time history of the temperature difference recorded from the thermistor under maximum intensity at a fluid depth of 20mm and at distances 20mm, 85mm, 150mm and 215mm from the light/dark boundary is presented. Temperature increased approximately monotonically for each run at respective thermistors positions.

Flow intrusions were detected shortly after radiative heating was initiated that became distinct with further heating. Each time the intrusion reached the thermistor a sharp spike in the temperature was noticed. The sharp spike

in temperature is attributed to warmer water travelling faster and catching up with the cooler and slower water forming a sharp front.
Identical trends were observed for the intermediate and low intensity experiments. Results are consistent with observations seen from the flow measurement. The main differences between results obtained at the three intensities are the magnitude of temperatures and possibly the timescale at which the intrusions occur.

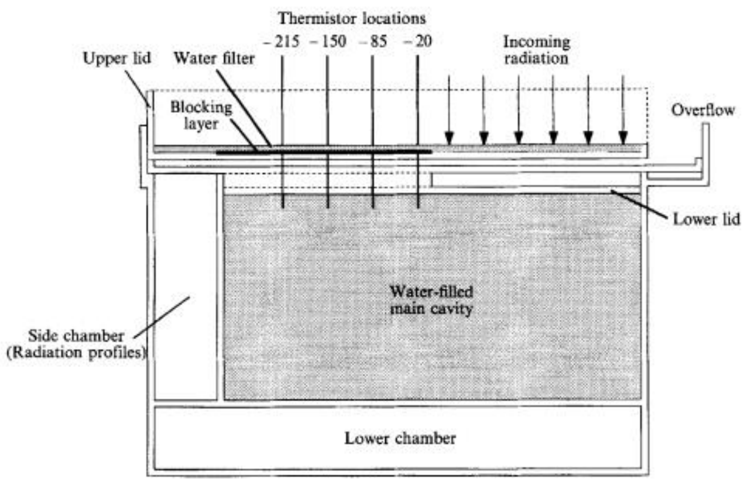

Figure 2: Schematic of the experimental setup showing the three comparments, two lids, thermositors and incoming radiation [16].

Natural convection induced by selective absorption of radiation was experimentally studied in laboratory experiments performed by Krishnamurti [17]. This study aimed to demonstrate that convection can occur in a stably stratified fluid layers. In this experiment a DC voltage was applied across the top and bottom boundaries of a fluid layer containing dilute solution thymol blue (a pH indicator), turns the water colour orange, turns yellow if water pH is low and turns blue if the pH is high [17]. At the start of the experiment the fluid layer was subjected to steady and uniform radiation incident from above with light from a sodium vapour lamp. Fig 4 presents the experimen-

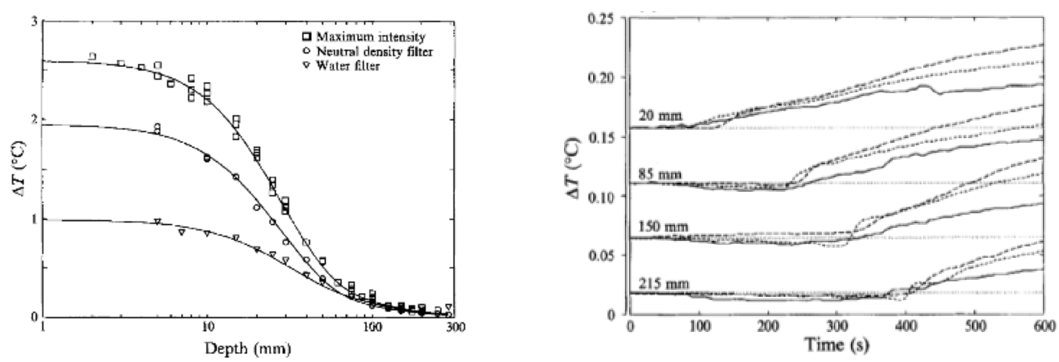

(a) (b)

Figure 3: (a) A plot of the measured temperature/depth data for the three experiments, acquired after the water had been heated for one hour. (b) The time history of temperature increase from the thermistor data taken a depth of 20mm in the shaded region for three repeated runs. [42].

tal set up and apparatus used in Krishnamurti [17].
Visual observations showed that radiation travelled through the orange fluid and was negligibly absorbed. In the blue fluid radiation was seen to be strongly absorbed. Convective instability was generated from the heating of the blue fluid, evident by the blue fluid rising into the warm upper layer. Penetration of the blue fluid into the upper warm layers continued to occur as long as the fluid layer remained blue and the generated temperatures exceed the temperatures in the layer above [17]. Radiative heating was observed to only occur in the blue rising flow and not in the orange fluid.
In Figure 5 an image obtained at Ra $= 8.0 \times 10^5$ shows a strongly stable stratified layer with convective plumes cluster penetrate the lower fluid layer but confined below that upper stable stratification is shown. For a weakly stratified layer, plumes extend further and collect into a large cluster which exists as steady coherent structures.

Experimental investigations for the unsteady natural convection induced by absorption of radiation in a triangular tank is reported in Lei and Patter-

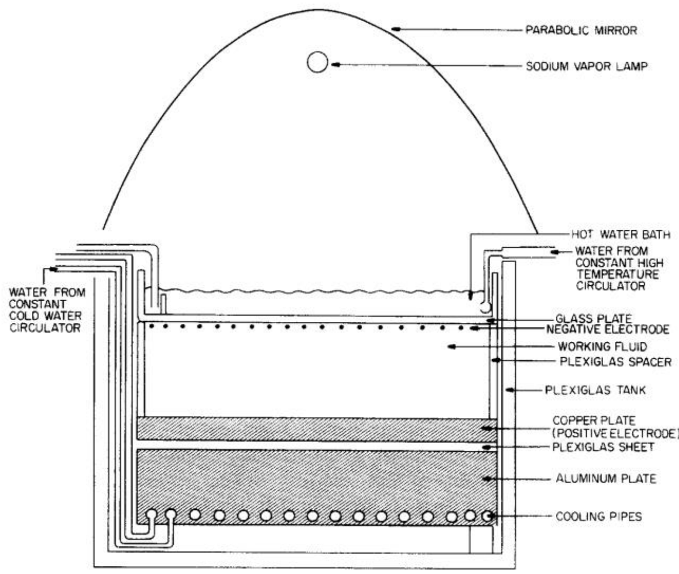

Fig. 1. Schematic diagram of the apparatus.

Figure 4: Schematic diagram of apparatus.

son [6, 7]. The aim of this experiment was to simulate the volumetric heating in a side arm in littoral waters due to solar radiative heating.
For the experiment a shallow water filled triangular tank with dimensions l=600 mm and h=60 mm with a sloping and absorptive bottom was directly illuminated by a theatre spot light source at the top surface.
Thermocouples situated at discrete locations along the sloping bottom measured fluid temperatures and fluid velocities were visualised using shadow technique. Fig 6 presents images of the water body at heating times 10s, 20s, 30s and 40s.
In Fig 6a, t=10s after the initiation of thermal radiation, the volumetric absorption of the incident radiation generated noticeable increase in water body temperature in downward direction. The non-absorbed radiation absorbed at the lower surface heats it and a thermal boundary layer is formed adjacent to the lower surface which continued to grow for maintained heating. At some stage when the thermal boundary layer became thermally unstable, thermal plumes are seen to grow out of the boundary as illustrated in Fig 6 b and c. In Fig 6d, further growth of the rising plumes within the lower fluid

column but confined below a stable thermal stratification is exhibited. Results demonstrate that thermal stratification of the water column and thermal plumes are important thermal features. The flow development is categorised by three distinct stages; (i) an initial stage marked by thermal boundary layer development (ii) a transitional marked by the existence of rising thermal plumes that extend out of the thermal boundary and into the fluid column and (iii) a quasi steady state stage. Authors suggested that their results obtained has not been previously been reported in literature. However, in spite of the significant findings reported the investigation, the experiment was limited to one set of the experiment test and was insufficient to draw a full picture of the flow. The set up did did not also permit a meaningful parametric investigation of this flow. The non linear temperature field and flow structures are consistent with previous studies.

The characteristic zones in penetrative convective mixing in a stratified fluid layer were reported for laboratory experiments of Maroni and Canedese

Figure 5: Unstably stratified tank and a shallow convective cluster and plumes taken for Ra = 8.0×10^5 [17].

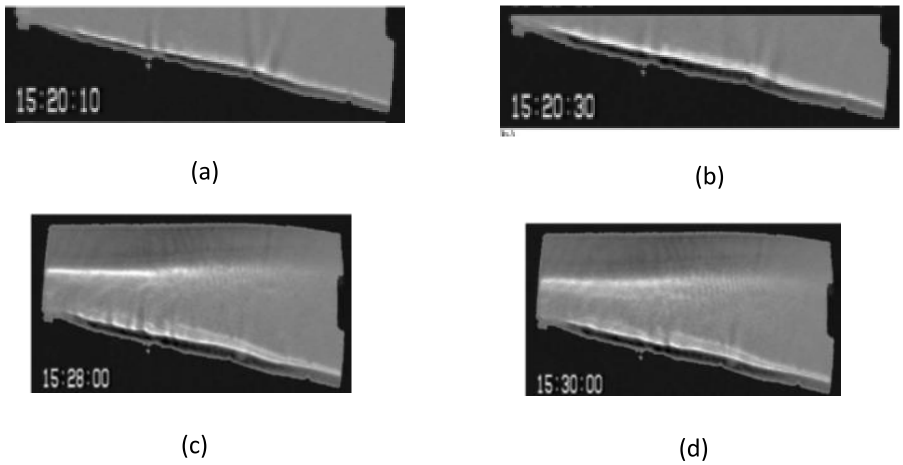

Figure 6: Shadowgraphs at (a) 10s (b) 20s (c) 30s (d) 40s [6]

[19].
A 1000 W arc lamp directly heated water contained in a prismatic tank with a square base of dimensions 0.41 $\times$ 0.41 m^2 and height of 0.40 m, insulated with Polystyrene sheets on all side walls. A beam stopper was used to control the depth of the illuminated area during the experiment.
Twenty-seven thermocouples placed along a vertical line measured the vertical temperatures and a second set of thermocouples placed along a horizontal line on the lower boundary monitored the horizontal temperature profiles and horizontal homogeneity.
Feature Tracking (FT) measured the fluid velocity along a vertical cross-section. Images of highly reflective tracers (pollen particles with average size of about $= 80\mu$m) were recorded using two monochrome 8-bit CCD cameras with a time resolution of 25 frames per second (fps)[19]. Fig 7 a-c, presents images captured for shadow graphs recorded at experimental time, t= 180s, 400s and 919s. From these figures development of the thermal plumes with time is illustrated and the extent of extension from the lower surface into a region of stable stratification is easily seen. Visualisation performed also investigated the movement and shape of the interface between an stable and unstable layers.

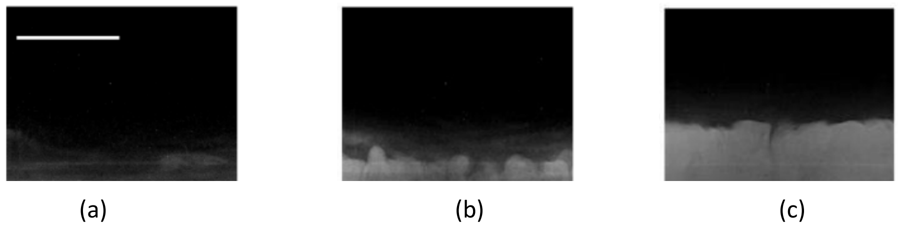

Figure 7: Visualisation of mixing layer evolution. Each snap shot corresponds to a progressive time (white line in frame is 10cm); (a) 180s, (b) 400s (c) 919s [19].

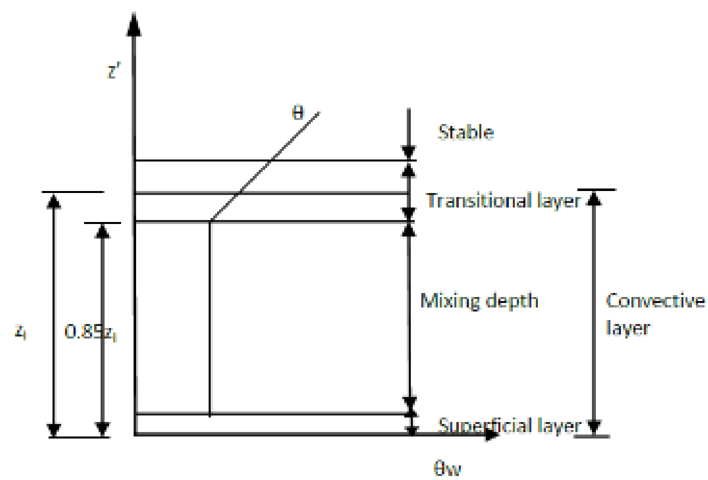

Figure 8: Schematic showing characteristic zones [19].

Characteristic zones for penetrative convection were identified in this study which shown in Fig 8:

i. Stable layer: is characterised by a stable temperature profile with constant gradient and zero convective heat flux .

ii. Mixing layer or transitional layer: Natural convection evident by the existence of narrow plumes extend out of horizontal surfaces.

iii. Boundary layer or mixing layer: Characterised with a typical thickness of about $0.85z_i$. The layer temperature and density profiles are constant. transitional layer, at around $0.85z_i < z < 1.2z_i$, the temperature profile increases and reaches a stable behaviour.

The flux passing through the interface between the mixing layer and the stable layer was play a fundamental role in characterisation and forecasting of water quality in shallow water layers [19].
Dore et al. [20] advanced Maroni and Canedese [19] earlier experiments by using three-dimensional Particle Tracking Velocimetry (3D-PTV) technique to investigate penetrative convection in stratified fluids.
Boundary layer experiments captured the evolution of the mixing layer and its growth with time.
Fig 9a shows the results of the measured temperature time history. The profile as shown changes with time and three distinct characteristic regions : (a) a negative gradient in the boundary region associated with the existence of the thermal boundary layer, (b) a uniform temperature in the region where mixing occurs and (c) a region above the mixing layer, where the temperature profile becomes a straight line of the initial stratification can be seen. Fig 9a presents the corresponding plot of the standard deviation of the vertical velocity component with time. The standard deviation very small at the beginning which later grew and covered a greater portion of the fluid depth as can be seen in Fig 9a. This finding supports previous results where the mixing layer associated with fluctuations in the measured velocity about a mean value. From the plot a sharp increase from the boundary with height can be seen.
A comparison of results showed that three-dimensional Particle Tracking Velocimetry (3D-PTV) technique is more accurate than a convectional scanning two-dimensional PTV for high tracer particle density. This is attributed to the fact that particles can be tracked directly in three-dimensional space rather than through matching of two-dimensional projections. Therefore, a three-dimensional PTV procedure would be more suitable for reconstructing a displacement field (i.e. particle trajectories) in both the mixing and the stable layer, allowing much more particles (> 1,200) to be tracked.

Bednarz et al. [21] combined Particle Image Velocimetry (PIV) and Particle Image Thermometry (PIT) techniques to experimentally investigate the

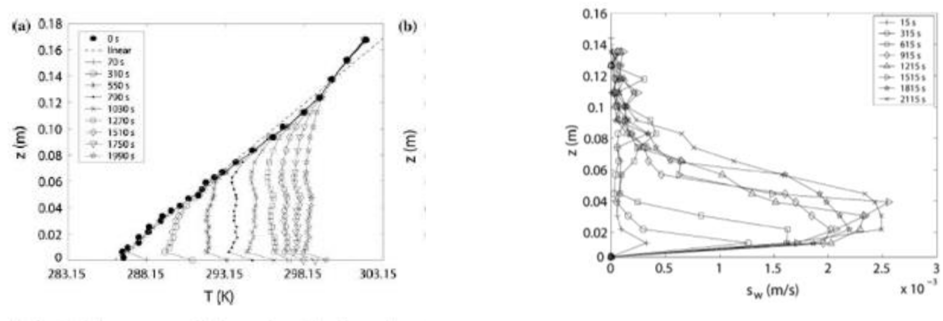

(a) (b)

Figure 9: (a) Observed vertical temperature (b) Standard deviation profiles of the vertical velocity at different test times [20].

unsteady natural convection in a water filled reservoir model subjected to periodic thermal forcing. Experiments were conducted in a reservoir with dimensions L=30cm, W=6cm and H=1.5cm; a wedge (inclination 0.1, horizontal length Ls=15cm, W =6cm and H=1.5cm) made from transparent Perspex. The central vertical cross-section of the flow domain was subjected to white light from a halogen lamp of a 150 W Liesegang 3000AF projector located about two meter from a mirror placed underneath the reservoir. External wall of the experimental reservoir were not insulated in order to allow illumination and visualisation of flow fields.

A quasi steady state natural convection within the trapezoidal reservoir whose temperature and flow fields are characterised by stable stratification of the water body during the heating phase and an unsteady mixing flow in the reservoir during the cooling phase [21].

Photographic images were captured using a high resolution 112.8 Mega Pixel (4368 $\times$ 2912 pixels) SLR digital camera (Canon EOS 5D).

Fig 10a shows images experimental images, extracted isotherms (Fig 10b) and velocity contours (Fig 10c) obtained from a periodic thermal forcing for Gr=3.52×10^4 and Pr=6.82.

Natural convective circulation in the reservoir changed direction when ther-

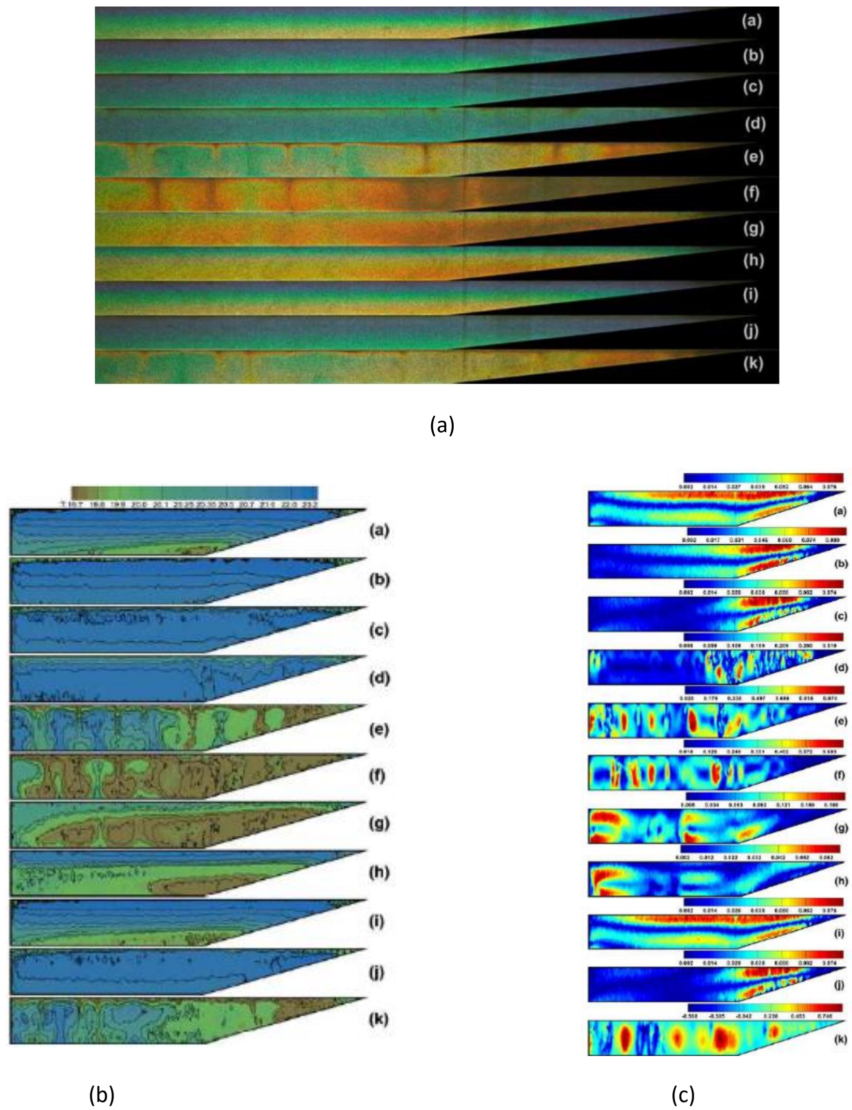

Figure 10: Experimental results (a) Experimental images of the observed flow at Pr=6.82 and Gr=3.52 $\times$ 10^4. (b) Isotherms extracted from the colour images in (a). (c) Velocity magnitude contours at different stages of the flow response to the periodic thermal forcing at Pr=6.82 and Gr=3.52 $\times$ 10^4.[21]

mal forcing switched from cooling to heating and vice versa. Observation of the thermal instabilities developed within the reservoir, reveal important mechanisms for breaking up circulation and initiating a reverse flow circulation in the water body when a switch of the thermal forcing from heating to cooling occurred.
Calculations for the horizontal flow rate exchange obtained from the velocity measurements showed the overall strength of the circulation in the heating phase is significantly weaker than that obtained in the cooling phase. Results obtained for the flow development suggested the findings in this paper to be relevant to cloudy atmospheric conditions on days when solar radiation is not available (cloudy conditions). Under such conditions the flow is solely driven by ambient temperature changes and the cooling effects dominates the convective heat transfer within the reservoir.

Naghib et al. [22] more recently, conducted laboratory scale experiments to study natural convection boundary layer in water-filled square cavity under radiative heating from a halogen lamp. The study was motivated by the interest in understanding the mixing driven by the daytime direct absorption solar radiative heating occurring in the near shore regions of lakes established stability properties. The experimental appartus and procedure fully described in Naghib et al. [22] and briefly discussed here. An square tank (140mm) assembled from double glazed glass side walls and black anodized aluminium bottom boundary was used. A 1000 W halogen lamp, with a colour temperature of 3000K and spectrum assumed to be similar to that for solar spectrum was used as the source of radiation.
The study simultaneously applied visualisation shadowgraphs and Particle Imaginary Velocimetry (PIV) techniques to visualise thermal plumes development due to induced instability. The authors highlighted the novelty in using concurrent PIV and shadowgraph technique for investigations for radiation induced natural convection of problem [22]. Fig 11 a-f presents the concurrent PIV/shadow graph images for a representative test run. These results can easily be matched with the different stages of flow development previously identified.
In Fig 11a and b shadowgraphs and PIV show the first stage associated with the flow development charaterised by no fluid flow and thermal boundary layer development. In Fig 11c images shows thermal features, plume-like structures consistent with the second stage flow development marked by the onset of thermal instability. In Fig 11d growth of the thermal plumes into mushroom shape plumes that extend into the fluid column towards the top

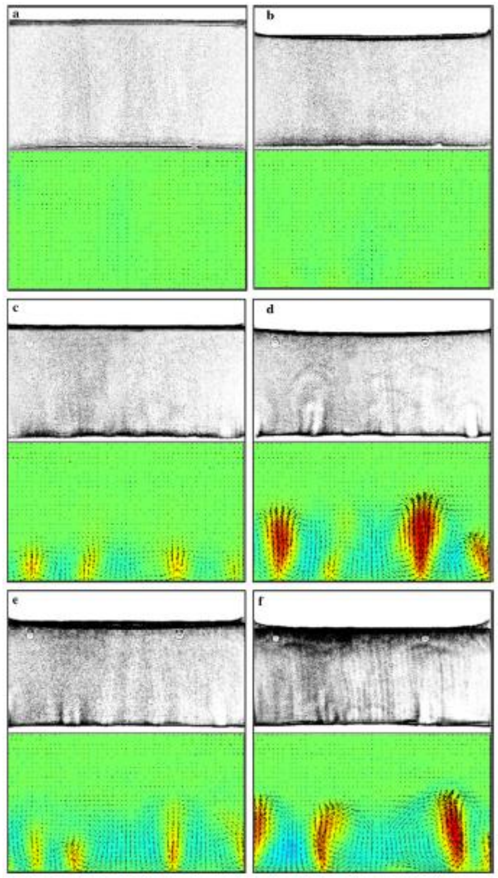

Figure 11: Concurrent PIV/shadowgraph images illustrating different flow stages. (a) 33 s. (b) 134 s. (c) 192 s. (d) 240 s. (e) 318 s. (f) 618 s.[22]

surface and impinge on the underside of the upper thermal boundary layer is shown. In the third flow development stage thermal plumes disappear and first and second stages are repeated in a cyclic pattern as illustrated in Fig 11e and f [22].

Thermal and flow features reported here are consistent with results of Lei and Patterson [6]. Direct comparisons between the experimental and scaling results were performed and were found to be in good agreement. Three dimensionality of the temperature and velocity field was also demonstrated which have provided a basis for comparisons between two and three dimensional flow behaviour.

Table 1 presents a summary of experimental work and experimental investigation for natural convection in enclosures driven by absorption of solar radiation. Reviewed experimental results show a good consistency and agreement amongst the many different. Therefore, results reported in experiments are sufficient in providing good insight to the physical process and the thermo-fluid transport. However a weakness for most of the studies is that simulation of the complex reality of the instantaneous incoming radiation intensity,is simplified by keeping a constant value from theatre and spot lights. In nature, the intensity of the incident solar radiation is variable and is dependent on the diurnal cycle, climate and cloud conditions [22].The source of radiation spectrum is considered to be a close approximation of the solar spectrum, however has been shown not to be identical. As such, the plume rise velocity could in the reality be of a higher order of magnitude, which could consequently lead to significant higher rates of mixing beneath the top thermally stratified layer than that investigated in the laboratory, owing to the nature of the Rayleigh numbers 10^{11} - 10^{12}, which are higher than that obtainable in the laboratory experiments [22].

3. Analytical (theoretical) analysis

Considerable number of studies on prediction models for radiation driven natural convection using analytical techniques have been reported.
Early studies of Estoque [25] derived equations give in Eqn 1-3) for estimating the rate of heating due to penetrative convection and the subsequent temperature of the environment due to near ground penetrative convection on strong solar heating days. In Equation 1 prediction of the heating rate strongly depends on a constant of proportionality (K) Tests on Equation 1 was performed using empirically derived data for the temperature difference and the heat flux. Results showed that as the temperature difference diminished the heating stopped. This demonstared a major limitation in its predictions. Eqn 1 was modified in order to improve the applicability for predictions. Eqn 2, the modified equation which included a term M(Z). Test using
Eqn 2 for the calculation of the theoretical local temperature using extrapo-

Table 1: Summary of the Experimental investigations on the radiation induced natural convection.

Author	Geometry	Method	Result and Remarks
Lei & Patterson [8]	Triangular	Shadowgraph visualisation technique.	Flow visualisation revealed an initial growth , transitional and quasi-steady stages of the flow development.
Walden & Ahlers [13]	Cylindrical	Thermocouples	Initial N(R) for R near Ra_c was independent of P. For P $\leqslant$1, two hysteresis loop formed, P$>$ 2 multistability observed. For large P onset of time dependent flow occurred much closer to R_c than in boussinesq systems.
Webb & Viskanta [15]	Rectangular	Copper constantan thermocouples, Mach-Zehnder interferometer	Hydrodynamic boundary layers observed at vertical walls, being thinner at the cooled wall. A convection regime prevailed with thin boundary layers at the vertical walls and a stagnant, stably stratified central core. Difference in interference fringe densities at the vertical boundaries illustrated the absorption of radiation in the fluid.
Coates & Patterson [16]	Rectangular	light source used in the experiments was the Prolite company's Profile. Spot theatre lamp, containing a 1000 W quartz globe. Thermometric FP07 thermistors. velocities were measured by a pattern tracking technique	flow (inertial), becomes viscous or energy limited, dependent on the relation between Gr, η, and l_E, (through A_E,). Convective regime flow regime is satisfied for η_*^6 A_E^{-2} $<$ Gr by the experiments. Validity of flow regime, and prediction of inertial and energy-limited velocity and time scales confirmed.
Krishnamurti [17]	Rectangular	A 35 W sodium vapour lamp consisting of a tube 1.3cm in diameter, 50 cm long, but doubled into a 25 cm long U-shaped tube, was placed along the focus of this parabolic cylindrical reflector. Heat flux meter	shallow convection plumes formed in a stably stratified fluid through the selective internal heating. Plumes in weakly stably stratified layers become organized into one large convective cluster.
Moroni & Cenedese [19]	Cylindrical	Thermocouples for temperature data and Laser Induced Fluorescence (LIF) and Feature Tracking (FT) image analysis techniques.	Pollutant dispersion phenomena are naturally described in the Lagrangian approach as the pollutant acts as a tag of the fluid particles. A matrix represents one of the possible tools available for quantifying particle dispersion during the evolution of the phenomenon.
Bednarz et.al [21]	Trapezoid	150W Liesegang 3000AF halogen projector lamp. PIV and PIT flow visualisation measurements. Thermochroamtic liquid crystals	Stable stratification of water during heating phase and unsteady mixing flow during cooling phase. Thermal instabilities break up circulation and initiates reverse flow after thermal forcing switching
Naghib et al. [22]	Square	Theatre spotlight with a 1000-W halogen lamp. Radiometer (LI-COR LI-250). Shadowgraph and PIV flow visualisation measurements.	Onset of convection, plume rise height, and plume rise velocity determined from PIV and shadowgraph images. Agree with previously published scaling results.

lated surface temperature and heat flux data combined with observed temperature data were performed.

Results revealed that Eqns 1 and 2 are best used for dry convection. When convection is accompanied by condensation a general method suitable for calculating the ambient, water vapour increase in the atmosphere due to penetrative convection, local increase in equivalent potential temperature for a conditionally unstable atmosphere and other related properties is required. Eqn 3 presents derived general equation [25] proposed. The strength of the method is dependent in the specification of M(Z) in terms of large scale situations and the physical characteristics of the Earth surface.

$$\left(\frac{\delta\theta}{\delta T}\right)_c = K(\theta_0 - \theta) 0 \leqslant Z \leqslant Z_E \tag{1}$$

$$\left(\frac{\delta\theta}{\delta T}\right)_c = KM(Z)(\theta_0 - \theta) 0 \leqslant Z \leqslant Z_E \tag{2}$$

$$\left(\frac{\delta\theta}{\delta T}\right)_c = \frac{I_i M(\theta_0 - \theta)}{\int_{Z_{\delta Z}}^{Z_{iE}} \rho(\theta_0 - \theta) dz} \tag{3}$$

where subscript c, indicates temperature change due to convection and K= $I = I_0/\int \rho(\theta_0 - \theta)dz$ is a proportionality constant, Z_i the height difference, Z_E is the equilibrium level. $M(Z) = 1 - Z/Z_E$ is arbitrary parameter proportional to mixing intensity.

Fig 12 presents results of the analytical computation plotted alongside a plot for a base case where M(Z)=1 against the height derivative of the observed heat flux. Satisfactory agreement can be seen between theoretical calculations and observed values for larger temperature differences at lower levels. The theory is seen to underestimate values at the lower end while overestimation is observed at upper level values. This is due to the fact that the proposed equations do not account for the effect of mixing between the thermal and the environment at lower levels.

Farrow and Patterson [5, 26] analytically investigated diurnal heating and cooling in a side-arm in a triangular domain with a small bottom slope. A two dimensional flow domain an infinite triangular wedge 0<z<-Ax' heated thermal forcefully by a uniformly distributed radiative source term on an open top surface. x is the horizontal coordinate measured from the tip and z' is the vertical coordinate measure in the positive direction. The lower surface of the enclosure was considered to be heated by absorption and re-emittance of residual heat flux of a triangular cavity.
The thermal forcing was modelled as an internal heating and cooling term

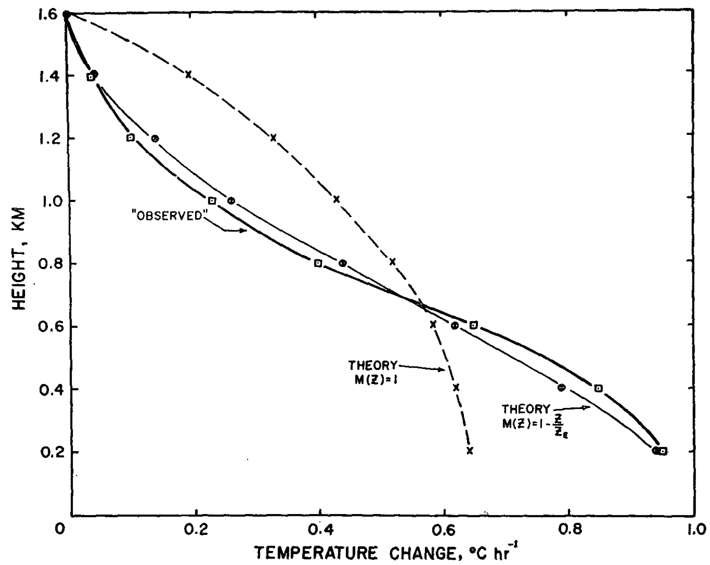

Figure 12: Comparison between theoretically derived values and observed temperature change [25].

integrated into a temperature equation of the form: $\frac{I_0}{\rho C_p A_x} cos(2\pi/P)^o C s^{-1}$. The method used an expanded series in A^2 shown in equation 4 for a dependent variable T and A parameter which appears as even powers in the boundary value problems according to Cormack et al. [27]:

$$T = T^{(0)} + A^{(2)}T^{(2)} + A^{(4)}T^{(4)} + ...\psi = \psi^{(0)} + A^{(2)}\psi^{(2)} + A^{(4)}\psi^{(4)} \qquad (4)$$

For brevity details of the derivation are omitted here. The solution is obtained solving partial differential equations and taking Laplace transform. The solution for the horizontal velocity is given by:

$$U^{(0)}(x,z,t) = -\frac{1}{96\pi x^2} sin(2\pi t)(z+x)(8z^2+zx-x^2)$$
$$-2x\sum_{n=1}^{\infty} \frac{1}{\beta_n^4 sin\beta_n}\Bigg((\beta_n cos(\beta_n z/x) - \beta_n cos\beta_n)(\frac{1}{2} + (cos\beta_n - 1)/\beta_n^2)$$

$$-(\beta_n cos(\beta cos(\beta_n z/x) - sin\beta_n)(1 - sin\beta_n/\beta_n)\Big)$$

$$\times\{\frac{(\beta_n/x)^2 cos(2\pi t) + 2\pi sin(2\pi t) - (\beta_n/x)^2 exp - (\beta_n/x)^2 t}{(\beta_n/x)^4 + (2\pi)^2}\} \quad (5)$$

where β_n are the non-zero positive roots of the equation $\sin\beta_n = \cos\,\beta_n$.

Asymptotic solution obtained from analytical equations which were supported by numerical simulation showed more rapid heating and cooling to occur in the shallow regions which lead to distinct transition from the shallow regions. The presence of a sloping bottom resulted in the flux being greater at the shallow end than at the deeper end.
Farrow and Patterson [28] presented results for a more realistic daytime heating model driven by internal buoyancy sources and a boundary flux by accounting for depth dependent absorption of radiation. The problem considered in the context of the near-shore transport question suggested that the model can be relevant to any buoyancy-driven flow in which competing stability effects are present. The model combined the principle of both the attic model and an initial exposition of the geophysical model. Equation 6 presents Farrow and Patterson's [5] analytical solution. Asymptotic solutions to the equations were obtained and the results were compared to experimental results in a reservoir sidearm in which a significantly good agreement was obtained.

$$\begin{aligned} T(y,t,h) = \frac{t}{h} - exp(y) + \frac{y^2}{2h} + y + \frac{1}{3}h + \frac{1}{h}(1 - exp(-h)) \\ -\frac{2}{h}\sum_{n=1}^{\infty}\Big[\frac{1}{(n\pi/h)^2} - \frac{1-(-1)^n exp(-h)}{1+(n\pi/h)^2}\Big] \\ \times exp\Big(-\Big(\frac{n\pi}{h}\Big)^2 t\Big) cos\Big((n\pi/h)^2\Big) \end{aligned} \quad (6)$$

Hattori et al. [29], extended Farrow and Patterson [5] analytical solutions to determine the depth of the mixing layer and height of thermal plume travel in a parallelpiped shaped fluid layer with small slope situations and negligible horizontal convection. The equation which is derived from the one-dimensional, inhomogeneous heat equation. The solutions obtained

showed that the equation satisfied conditions at an initial stage temperature T_1, but struggled to resolve unsteady boundary conditions introduced after the onset of instability. Vertical fluid temperature distributions (T_1) before and (T_2) after the onset of instability in a deep water layer with surface stratification is shown in Figure 13. Proceeding the onset of instability is an unsteady unstable flow characterised by bursting of buoyant plumes from the bottom boundary layer. Following the onset of thermal instability, the bottom boundary layer thickness becomes reduced due to a significant amount of heated fluid being lost in the form of rising plumes and limitation in the diffusive growth due to induced convection [29]. The occurrence and bursting of thermal plumes leads to homogeneity of fluid temperature over the plume height determined by the location of the point of neutral buoyancy. The surface stable layer remained stratified and is not destabilised by the boundary layer instability.
Fig 13 shows a schematic of the theoretical model plot defining a plume penetration height h_m. The plume rise height as shown by previous studies is determined by the thermal stratification gradient [29]. From the plot the following was inferred: (1) The vertical temperature gradient over the lower mixed layer column significantly reduced as the temperature distribution became homogenised due to plume activity. (2) The thickness of the lower boundary layer is insignificant compared to the total lower mixed layer thickness. (3) Temperature distribution over the lower mixed layer can be assumed uniform.

3.1. Scaling analysis

Scaling analysis has also been used by various researchers to study flow instability in radiation-induced natural convective flows with shallow water filled reservoirs, relevant to the bouyancy flows found in littoral regions. [9, 10, 30, 31].
Lei and Patterson [9, 18] established scales to quantify the flow properties for flow regimes and describe flow states for different parametric settings in a triangular reservoir subjected to solar radiative heating. The study considered a two dimensional wedge of length (L) and maximum depth (H) whose top surface was directly heated by solar radiation. The sloping bottom surface was considered a black and capable of absorbing all the non absorbed radiation reaching it. Non slip conditions were applied at the bottom wall, end wall and at an open top surface.
From the scaling analysis possible flow stages of development dependent on

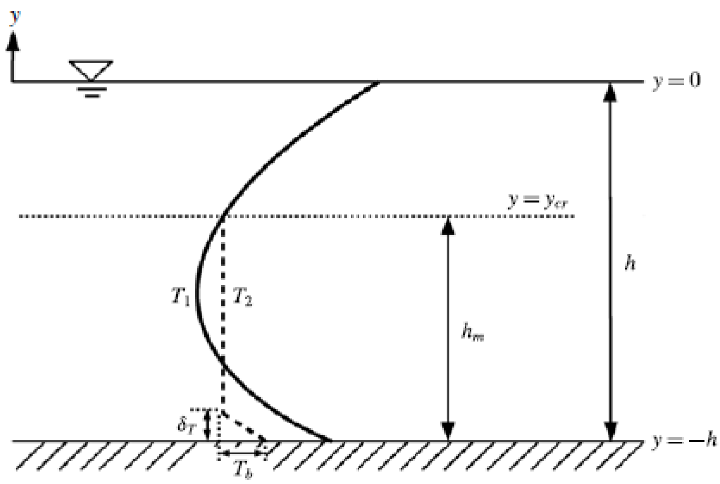

Figure 13: Schematic showing the bottom thermal boundary layer and the lower mixed layer thickness (h_m) with typical temperature distributions before (T_1) and after (T_2) the onset of instability in relatively deep waters [29].

the Rayleigh number were identified and described . The flow development stages were classified as conductive and convective/transitional and established scales were used to quantify their flow properties.

In an improved scaling analysis study conducted by Mao et al. [10], detailed scaling analysis for flow in a triangular reservoir with relatively large bottom slopes at high Rayleigh numbers were reported. The study aimed to reveal more detailed flows properties that was not captured by previous analysis. Properties of the thermal flow development were divided into three sub-domains, with the dominant mode of heat transfer changing from conduction into stable convection and subsequently into unstable convection as offshore distance increases. This scaling analysis demonstrated the extent of the unstable region and the onset time for instability at varying offshore distances. However, capability of the scaling analysis was limited in revealing further stability properties of the unstable region. With reference to a horizontal position, investigators derived critical function for the Rayleigh number from the scaling analysis used to identify the distinctness and stability of a thermal boundary layer. Four possible flow scenarios identified were found to be dependent on the bottom slope and the maximum water depth. For

the respective identified flow scenarios, the flow domain consisted of multiple sub-regions with unique characteristic thermal and flow features dependent on the Rayleigh number. The dividing points between neighbouring subregions were determined by direct comparisons of the critical functions of the Rayleigh number and a global Rayleigh number. Position-dependent scales were also established to estimate flow properties in different subregions. Author's suggested that a power spectrum of the time series of flow properties would vary with offshore distance and would provide better insight into the variation of mixing and transport with offshore distance.
The characteristics of instability in the transitional flow regime based on spectral analysis was reported by Mao et al. [10]. Harmonic frequency modes were observed for relatively low Rayleigh numbers. The power and prominence of instability at higher frequency modes increased with offshore distance and Rayleigh number. It was suggested that for a given offshore distance the frequency modes of instability are the same over the local depth, but the prominence of higher frequency modes increased with depth.

Linear and non-linear analysis have also been applied to study radiation induced natural convection in reservoirs by different researches. Amongst these include works of Farrow and Patterson [28]who performed a linear stability analysis to study an asymptotic base flow with the bottom slope approaching zero, where a critical Rayleigh number for instability was derived as a function of the offshore distance. The analysis was however unable to characterize the instability properties in more developed flows.
Hill [32], applied linear analysis and conditional nonlinear analysis based on the nonlinear energy theory to Krishnamurti's [17] study. The study defined a concentration based quadratic expression [32] that generated results consistent with a linear model internal heat source used by Krishnamurti [17], within defined parameter ranges. The linear theory was found to be only accurate enough to predict the onset of convective motion when the model for the internal heat source is predominantly linear. This is attributed to the presence of significantly large regions of potential sub-critical instabilities.
Harfash [33, 34] extended the linear stability and the nonlinear energy stability analysis of Hill [32] to three dimensional simulations.
In this study the, onset of convection predicted in Krishnamurtis model [17] was explored to determine sub-critical regions where the linear instability and non-linear stability thresholds significantly deviated.
Three dimensional governing equations were solved using an efficient, stable,

and accurate finite difference scheme using a velocityvorticity formulation combined with a staggered grid. Implicit and explicit schemes used enforced the free divergence equation used in the study.

Three different patterns dependent on the Rayleigh number (Ra) were obtained for convection: For $\mathrm{Ra}^2 < \mathrm{Ra}_L$, the temperature, velocity, vorticity and potential perturbations became negligible and the solution for a steady state, before the linear thresholds are reached was obtained. The time required to reach the steady state increased as the Ra^2 increased. For R^2 is close to Ra_L , solutions tend to a steady state which is different to the basic steady state for $\mathrm{Ra}^2 > \mathrm{Ra}_L$ the solution do not attain any steady state and oscillates.Ra_L is a thermal Rayleigh number

For three dimensional simulations, the inherent nature of the linear theory only provided boundaries for instability, but did not predict anything about instability, because of the presence of non-linear terms. For the non-linear stability theory full assessments of any regions of subcritical instabilities can be made. Therefore the non-linear stability theory is considered more desirable than the linear stability theory when applied to predict the stability analysis for the radiation induced convection in a three dimensional domains.

Hattori [35] highlighted three common approaches are commonly used in transient stability of penetrative convection induced by internal heating : the amplification theory, the frozen time model, and the propagation theory [35], for a stability analysis in transient systems [35–38].

The amplification theory requires specification of an initial arbitrary condition for velocity and temperature a priori and directly solves a linearised equation as an initial value problem. A major weakness of this model is its need for physically reasonable initial conditions that must satisfy the specified boundary conditions.

In a frozen time model and propagation theory, linearised equations are reduced to a system of Ordinary Differential eigenvalue problems. Both methods do not depend on the arbitrariness due to the specification of initial conditions inherent, as in the case of amplification theory.

The frozen time model and the propagation theory are used to investigate the stability properties of the flow. Frozen time model and propagation theory methods are computationally less expensive than an amplification theory analysis [35].

The linear and oscillatory behaviours of the natural convection boundary layer induced by the absorption of incident radiation in response to constant and time-varying (ramp) thermal forcing using linear theory and direct stability analysis is reported in Hattori et al. [36]. Based on a quasi-static linear stability analysis the fastest growth mode and its corresponding temporal growth rate was determined. Findings are in excellent agreement with results for the direct stability analysis previous numerical simulation. The time and frequency scales of the unstable bottom thermal boundary layer derived via a local Rayleigh number analysis revealed the boundary layer response to the time-varying thermal forcing is in equilibrium with the forcing intensity at each instant of time [35].

4. Numerical studies for natural convection induced by volumetric absorption of solar radiation

Webb and Viskanta [39] performed two-dimensional simulations for the natural convection in a geometry where the primary driving force for the natural convective motion is the volumetric absorption of thermal energy. Simulations were carried out in a two dimensional vertical semi transparent fluid layer bounded by rigid solid walls on all sides.The top and bottom boundaries were assumed to be rigid and adiabatic. A constant isotopic incident solar radiation was imposed at one of the vertical wall which was transparent and transmitted the radiation. The incident radiation penetrated the fluid layer and volumetrically heated it in the process and subsequently developed a buoyancy driven flow. The opposite wall were considered to be opaque and at a constant temperature.

Two-dimensional (non-dimensional) mass, momentum and energy equations with a radiative divergence flux term that accounted for the depth-dependent absorption of solar radiation based on a single weighted absorption coefficient was solved by Finite Element Method. Governing equations were discretised using the control volume scheme of Patankar while the SIMPLER algorithms coupled the pressure and momentum [39]. The numerical model was validated against previous experimental investigations of Webb and Viskanta [39] and good agreement was obtained between results.

Numerical results were presented in the form of isotherms, streamline and line plots. Fig 14 a-c shows isotherms, streamline and local convective heat flux for a representative simulation at Ra=10^7 . The heat transfer and fluid flow in this study was observed to be different from those seen in differential heated cavity problems. A direct comparison between the numerical results and interferograms obtained in previous experiments reveal identical features.

The effect of defined parameters; modified Rayleigh number (Ra), Prandtl number (Pr), fluid layer opacity, aspect ratio, wall reflectivity and heat loss on natural convection were studied. At high Rayleigh numbers flow is seen to completely lose centrosymmetry. As the the modified Rayleigh number increased the existence of conduction, transition and boundary layer regimes are evident. At low Pr number conduction is of greater importance while convection dominated at high Pr numbers. Increasing fluid layer opacity promoted the development of a boundary layer adjacent the transmitting wall where very high thermal energy is deposited. Increased aspect ratio resulted in a reduction in a stagnant central core in the boundary layer regime. Decrease in the convective heat loss and increase in opaque wall reflectivity slightly promoted convective flow.

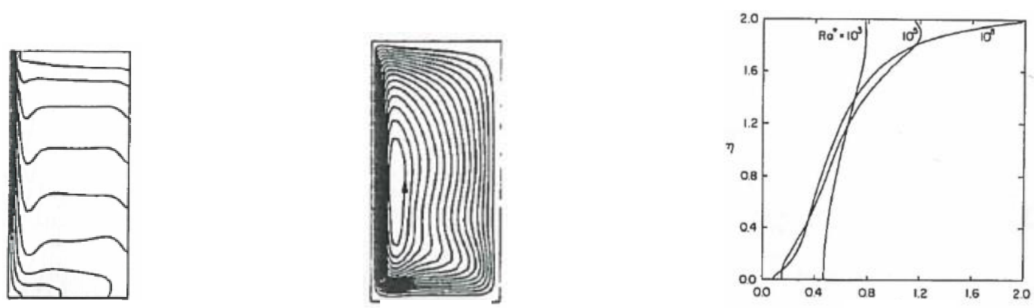

(a) (b) (c)

Figure 14: (a) Isotherms for temperature distribution (b) Streamlines for slow structure at for Ra=10^7 (c)Local convective heat transfer flux at the isothermal wall for Ra=10^3 $10^5$and 10^8 [15] .

Onyegegbu [40] performed two-dimensional simulations for the solar radiation natural convection in stagnant water layers. The study considered a water filled rectangular tank of depth (H) and width (2W), insulated on vertical side walls and bottom boundary and subjected to a time variant solar radiation at the open top surface. Convection was assumed to be two dimensional and flow is considered to be symmetric about the centre plane. The

model solved two-dimensional governing partial differential equations using Finite Difference Methods. An unconditionally stable alternating direction implicit method was applied to solve parabolic equations. The Non-linear convective terms were represented using second up-wind differencing methods. The radiative heat source was obtained from solving the Radiative Transfer Equations using a P-1 approximation.
Results obtained showed the induced natural convection set in the form of two counter-rotating eddies of unequal strength which has significant influence the temperature field of the fluid layer. This phenomenon occurred for Grashof numbers as low as 10^3. Effects of parameters; $10^3 \leqslant \mathrm{Ra} \leqslant 10^8$; $0.01 \leqslant \mathrm{Pr} \leqslant 1000$, $1 \leqslant \mathrm{A} \leqslant 5$ and $0 \leqslant \mathrm{Bi} \leqslant 5.0$ on temperature distribution, local heat transfer and flow structures was performed. Results revealed that convection is promoted by low fluid optical thickness and increased albedo. The effect of the bottom boundary emissivity was significant only at low and intermediate optical thickness where low boundary emissivity suppressed convection.
Flow pattern characterised in three different regimes as intermittent convection, steady state convection and free-convection were reported in the a numerical study of Verevochkin and Startsev [41]. The result was reported for the thermal convection in a horizontal water layer cooled from the top and absorbing solar radiation [41]. The flow transition occurred for different combination of the ratio of the downward solar radiation flux at a depth (J_0) to heat flux through the interface (Q), and at almost the same Rayleigh number.

Two and three dimensional numerical investigations of unsteady natural convection induced by absorption of radiation were performed for shallow water filled triangular enclosures with sloping bottoms and subjected to solar radiative heating [7–9]. The study was carried out to understand buoyancy driven flows with respect to the daytime natural convection in a side arm and in littoral regions [6–9].

Two and three dimensional momentum, energy and conservation equation Governing equations were solved using a Finite Difference scheme. A standard Second Order Central differencing scheme is used for spatial derivative. Non linear terms in the governing equation were solved using the second order upwind scheme. Details of the numerical schemes can be found in [8, 9]. Fig 15 shows results from the two dimensional simulations at times corresponding to 25s, 328s, 5302s and 5049s respectively. Images reveal features consistent and can easily be matched with the early, transitional and a quasi-

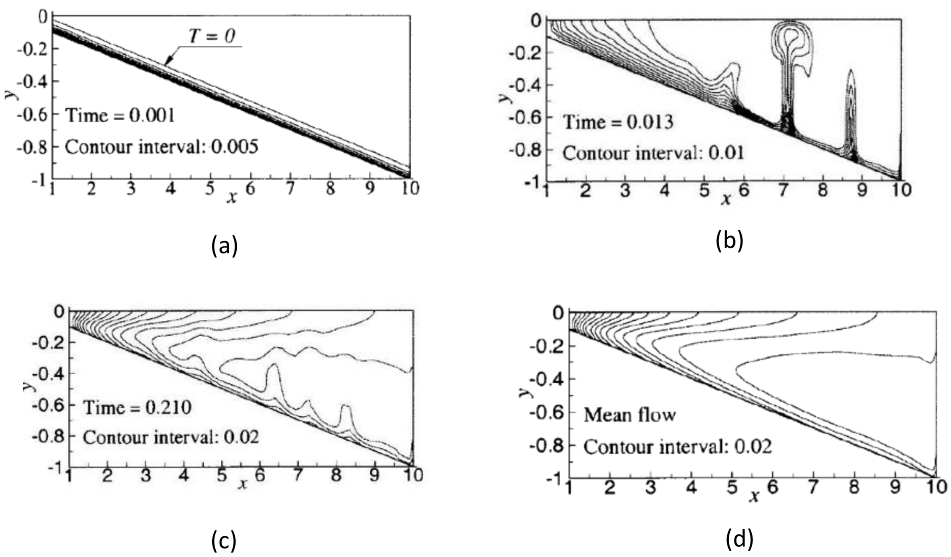

Figure 15: Two dimensional temperature contours during various heating times (a) t=0.001 (t=25) (b) t=0.013 (328s) (c) t=0.21 (5302 s) (d) t = 0.200 (5049s) [7].

steady flow stages. Good agreement between the two-dimensional simulation and observations from a flow visualisation experiment was obtained.

Fig 16a-c presents images for the corresponding three dimensional simulated iso-surfaces for radiation induced natural convection in a triangular enclosure for various time steps. Iso-surfaces can be matched with the three stages of the flow development: an initial stage, a transitional stage and a quasi-steady stage. The heat transfer at the initial stage was dominated by conduction from the sloping bottom. The transitional stage started with the onset of instabilities, and the quasi-steady state was characterised by steady growth of a spatially averaged temperature. The results were also found to be consistent with observations from a flow visualisation experiment and the two-dimensional simulations. Fig 16d, presents a plot for the two and three dimensional time histories for the integrated horizontal heat transfer rate from two dimensional and three dimensional simulations. While the previously identified three stages of flow development can be easily seen for these plots, discrepancies in time time-scales and the duration of occurrence exist. This discrepancies between plots is attributed to non inclusion of the azimuthal orientation in the two dimensional simulation.

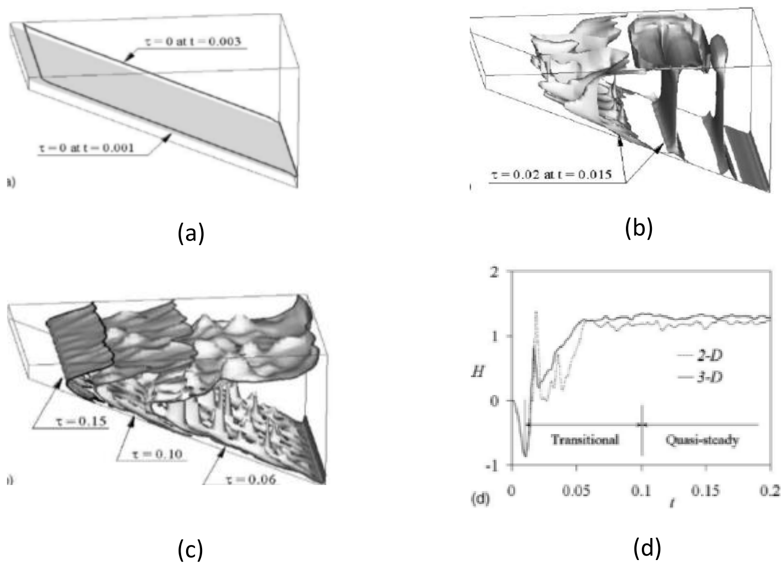

Figure 16: Three dimensional temperature iso-surfaces during various heating times (a) t=0.001 (t=25s) (b) t=0.015 (t=379s) (c) t=0.21 (t= 5302s) (d) Time series of integrated horizontal heat transfer rate [8].

In recent studies, three-dimensional simulations and scaling analysis for the natural convection in reservoirs filled with water and subjected to solar radiation was reported by Hattori et al. [29, 35]. The geometry studied is considered to be relevant to deep water bodies subjected to top solar radiative heating [29].

Direct Numerical Simulations (DNS) were applied to solve the coupled three dimensional mass, momentum and energy equations. An internal heat source term in the governing equations is defined as $s(y) = \frac{I_0}{\rho_0 C_p}\eta e^{\eta y} - I_0\rho_0 C_p h$, where

I_0 is the solar intensity at water surface, C_p is specific heat capacity, η is the bulk attenuation coefficient.

The governing equations was solved using a non-staggered, Cartesian mesh, Finite Volume code (SNS code), developed in Fortran90 language. The SNS code is generally based on a fractional step method, with Adams Bashforth and Crank-Nicolson time discretisation schemes used for the advection and diffusion terms. Second-order central differencing schemes are used for the spatial discretisations of diffusion and advection terms, while a Bi-Conjugate Gradient Stabilised method (BICGSTAB) with a SIP preconditioner is used for Poisson pressure correction.

Results described a non-linear temperature distribution consisting of two distinct adjacent layers; an upper stratification region due direct absorption of radiation, and an unstable boundary layer due to the absorption and re-emission of the residual radiation by the bottom surface [29]. The existence of a non-linear temperature stratification is seen to physically limit the thermal plumes maximum height and mixing depth. In other words the non-linear temperature stratification was considered to determine the penetration length scale of the plumes and the lower mixed layer thickness. On the basis of theoretical calculations the lower mixed layer thickness is suggested to be equal to the attenuation length of the radiation [29].

Fig 17 presents temperature and flow contours for Ra = 1.27×10^9, hη = 0.72 and dimensionless time, t = 0.0026 - 0.0039 . In Fig 17a, temperature iso-surfaces show a thermal boundary laying approximately parallel to the bottom boundary. In Fig 17b, thermal instability is introduced within the boundary layer illustrated by evolution of thermal plumes. In Fig 17c, thermal plume emerge from the thermal boundary, while in Fig 17d thermal plume fully develop and extend into the fluid column. In Fig 17e and Fig 17f show the Iso-surface of vorticities for the x and z components at position x = z = 19.4. Dark and light patterns depict positive and negative vorticities. Iso-surfaces of vorticities also indicate the formation of convective rolls with a distinct dominant wavelength in each direction. These results are supported by experimental and scaling analysis results reported in previous sections.

Turbulent natural convection simulations for the daytime heating and night time cooling in a shallow tetrahedron domain was reported in Dittko et al. [43]. The tetrahedron domain studied was considered to be a more realistic representation of three-dimensional approximation of a lake or reservoir sidearm compared to a previously used two [7] and three-dimensional tri-

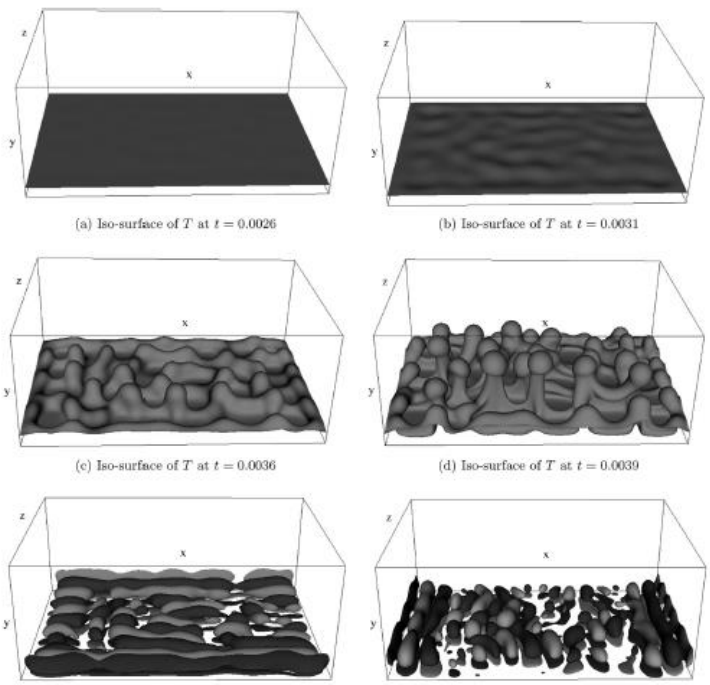

(a) Iso-surface of T at $t = 0.0026$ (b) Iso-surface of T at $t = 0.0031$

(c) Iso-surface of T at $t = 0.0036$ (d) Iso-surface of T at $t = 0.0039$

(e) Iso-surface of ω_x at $t = 0.0026$ (f) Iso-surface of ω_z at $t = 0.0026$

Figure 17: Flow structures for a case with Ra=1.27×10^9 [29].

angular domain reported previously. The two dimensional reservoir model studied consisted of a region with a sloping bottom and one with a uniform water depth. The model has a total length L, maximum water depth of h and a slope inclination of A =0.1.

Governing equations were solved by finite volume, fractional step, pressure correction method in a A PUFFIN (Particles IN Unsteady Fluid Flow) solver. Fourth Order central difference scheme with the ULTRA flux limiter was used for the advection scheme. Time stepping was based on a second order hybrid Adams-Bashforth/Crank-Nicolson scheme. A staggered Cartesian grid is used along with the localised dynamic Smagorinsky model to account for subgrid scale turbulence effects [43].

Fig 18a shows temperature contours in a tetrahedron under solar radiation with Ra=35,000 while shows Fig 18b velocity contours in the x-direction in a tetrahedron subject to cooling with Ra=1.6×10^5.

A thermal boundary layer formed just above the bottom surface is seen from this plot. In Fig 18a conduction heat transfer is dominant close to the domain tip which is demonstrated by the vertical contours in the figure. Curved contours occurring away from the shallow tip illustrate the presence of a convection dominated flow. The flow seen maintained the expected general trend to travel up along the sloped bottom boundary and along the surface. The result supports the assumptions made in the scaling analysis for the two dimensional flow in the x-direction.

Fig 18b the contours shown indicate that on unstable flow occurs. A two return flow is exhibited with the large area of the domain and a flow down the bottom slope occurs over the entire length of the domain. The flow indicates a strong volumetric transfer rate to and from the shallow tip down the bottom edge of the domain. Effects of end wall as also shown to have a strong effect of flow.

Calculations for the horizontal heat transfer and volumetric flow rates revealed significant changes to the flow and introduced some complex features such as helical flow towards and away from the tip.

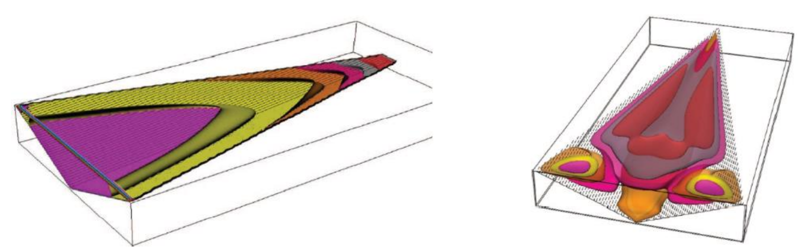

(a) (b)

Figure 18: (a) Normalised mean temperature contours at intervals of 7.5 in a tetrahedron under solar radiation with Ra=35000 (b) Contours for the velocity in the x-direction in a tetrahedron subject to cooling with Ra=1.6×10^5 [43].

Numerical simulations concerned with the transient flow response in a reservoir model subjected to periodic heating and cooling (thermal forcing) at the water surface was reported by Bednarz et al. [44–46]. The study was concerned with understanding of the flow mechanisms and prediction

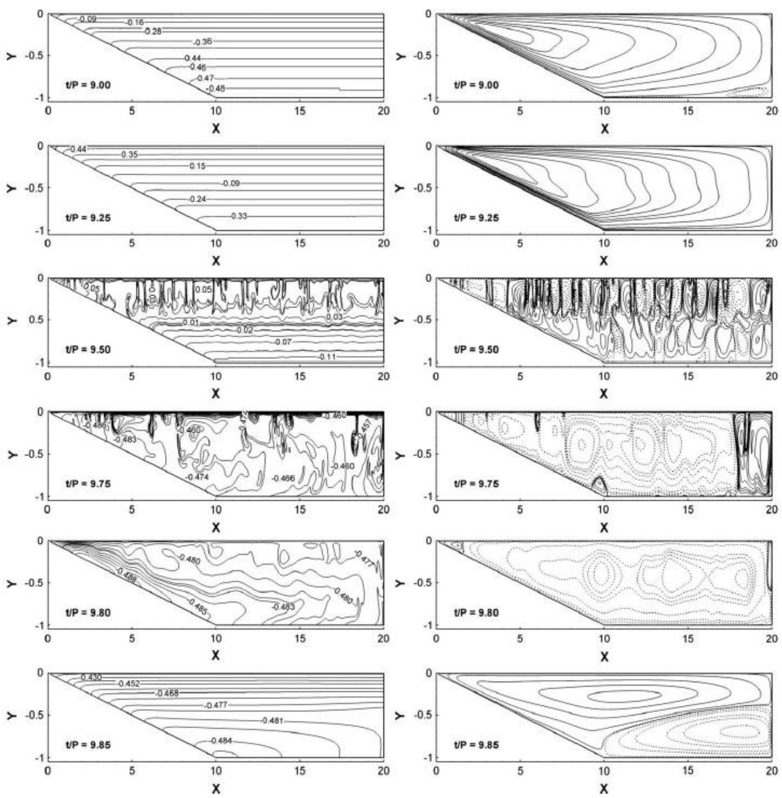

Figure 19: Different stages of the flow response to the diurnal thermal forcing in shallow waters of a reservior at Gr=10^7. Left: Isotherms, right: Streamlines [44].

of the transport of nutrients and pollutants across reservoirs. The overall objective of this study was to advance previous numerical investigation for a reservoir model with thermal forcing imposed at the top surface. Periodic thermal forcing considered for this simulation is obtained by varying surface temperature which estimated the effect of varying ambient temperature with no radiation input as could be experienced during cloudy atmospheric conditions.

Dimensionalized governing equations were solved numerically with Finite Volume method with a double precision solver. For all calculations a second-order time formulation was employed. Spatial derivatives were solved using a third-order MUSCL scheme obtained by combining a central differencing scheme and a second-order upwind scheme. The SIMPLE algorithm is used for the Pressure velocity coupling.

Fig 19 presents the isotherms (left column) and corresponding streamlines (right column) at representative times over a typical diurnal cycle for Grashof numbers (Gr)=10^7.

Stable stratification of the water body during the heating phase and unsteady mixing flow in the reservoir during the cooling phase was obtained. The unsteady flow structures and stable stratification obtained in the numerical simulations are identical to those observed in experiments [21] carried out in a reservoir model cooled and heated from above in diurnal cycles. The development of unsteady convection described was based on experimental flow visualisation and quantitative temperature and velocity measurements using thermo-chromic liquid crystals. Developed thermal instabilities destroyed the residual circulation and initiated a reverse flow circulation in deep water when the thermal conditions changed from heating to cooling. For sufficiently strong cooling, a clear undercurrent was formed which drove cold water to the deep region of the reservoir. Heating from the water surface generated a stable large-scale convective roll. Results also showed that the primary convective circulation in the reservoir changes its direction (flow reversal) when the thermal forcing changes from cooling to heating and vice versa. The time lag of the flow response to the change of the thermal forcing from cooling to heating depended on the strength of thermal forcing characterised by the Grashof number.

The calculated horizontal exchange flow rates from the velocity fields showed the overall strength of the circulation in the heating phase is significantly weaker than in the cooling phase. Thus suggesting that during cloudy conditions, the cooling effect dominates the convective motion in reservoirs.

The numerical results also presented indicated that the convective motions in reservoirs in diurnal cycles are very important from environmental and ecological points of view. Water circulation driven by horizontal thermal gradients may cause the transport of small, suspended pollutants, biological particles or dissolved constituents into or from deep water regions and thus plays a significant role in determining water quality. The paper however, considered only numerical results of convective motion in diurnal cycles and recommended further study of particle transport to help incorporate relative phase and motions of particles into calculation and applied to the ecological transport models.

Amber and O'Donovan [47] presented numerical simulations for the natural convection induced by direct absorption of concentrated solar radiation in molten salt filled enclosures for height to diameter ratios (H/D) of 0.5, 1 and 2 and Rayleigh numbers 10^7 - 10^{11}. The domain studied was made up of fluid cavity bounded by rigid adiabatic vertical walls, a heat-conducting bottom wall of finite thickness and an open adiabatic top surface, directly irradiated by a non- uniform concentrated solar flux. The simulation was conducted for the particular case that a salt volume is first heated by direct absorption of solar radiation and then by contributions from the lower boundary heated by the absorption of the radiation transmitted to it.

Time dependent two dimensional Navier Stokes Governing equations that included a depth dependent volumetric heat source was solved by Finite Element Method. Second-order and linear elements discretisation were applied for the velocity and the pressure field, (P_2+P_1). An unstructured mesh consisting of triangular mesh elements is adopted in the simulation to account for the variability of the formed thermal plumes and its occurrence at arbitrary locations [47]. The study also considered the temperature dependence of the thermophysical properties of working fluid. A nonlinear temperature profile consisting of a hot stable stratified fluid above a cooler convecting layers where thermocapilarity and buoyancy effects are evident was observed. Fluid flow development in the lower layer is found to exhibits three stages. Natural convection was found to decrease with increasing aspect ratio and increased with increasing Rayleigh number. The Nusselt-Rayleigh number relationship was found to not be linear.

Fig 20 shows the time averaged temperature contours, averaged over in the transitional stage for values: (a) Ra = 107, (b) Ra = 10^8, (c) Ra = 10^9, (d) Ra = 10^{10}, (e) Ra = 10^{11} at H/D = 0.5, 1 and 2. At H/D = 0.5, plume penetration height and the intensity of plume occurrences increased with Ra. The flow in the lower layer exhibited an increasingly complex behaviour with increased Ra. Observations for H/D = 1 and 2 reveal that for each aspect ratio increased flows are found to occur with increasing Ra. From these plots it can also be seen that fluid flow corresponding to a particular Ra decreases with increasing aspect ratio.

Amber and O'Donovan [47] investigated the effect of inclination angle ($0 < \phi < 60^o$) natural convection in a molten salt-filled enclosure induced

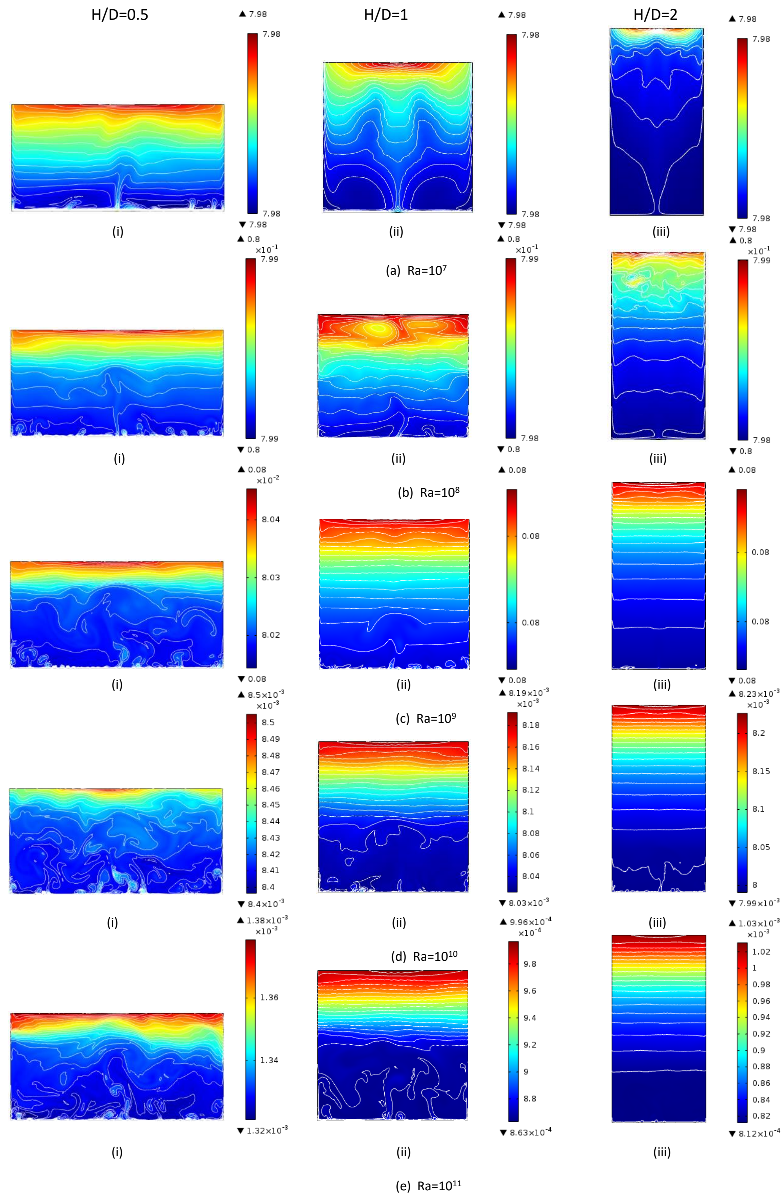

Figure 20: Time averaged temperature contours excluding the quasi steady regime at H/D=0.5 for Rayleigh numbers a) Ra=10^7 b) Ra=10^8 c) Ra=10^9 d) Ra=10^{10} e) Ra=10^{11} for H/D=0.5 (left column), H/D=1 (middle column) and H/D=2 (right column) [47].

by direct absorption of non-uniform concentrated solar radiation. A two-dimensional inclined enclosure with H/D = 1, whose vertical walls were inclined at an angle to the gravity vector was considered. All boundary walls were assumed to be rigid and adiabatic except for the top boundary which is an open stress-free boundary. Bottom boundary is of finite thickness (dx), and absorb all radiation reaching it. The lower boundary then heats the plate and drive natural convection. The working fluid (KNO_3-$NaNO_3$ salt), within the domain walls is initially at rest and temperature T_0. At time t =0, a non-uniform concentrated radiation flux is imposed and thereafter maintained.

The inclined geometry is identical to that used in [48] in every respect. The governing equations which includes volumetric heating source is solved using the Finite-Element Method with appropriate boundary conditons as reported in used in [48].

The temperature isotherms and corresponding fluid velocity contours are presented in Figure 21a e for angles of inclination, ϕ= 0^o, 15^o, 30, 45^o, and 60^o at t= 1250s, a time within the transitional regime where thermal plumes are evident and convective heat transfer is the highest.

Features at zero inclination have been discussed in the previous section and in Amber and O'Donovan [47]. For inclination angle (Fig 21b) ϕ= 15^o, the effect of this inclination angle on non-uniform temperature profile can be seen. Visual inspection revealed a reduction in the hot stratified layer thickness. Thermal plumes extended further into the fluid column than at ϕ= 0^o but remained confined by it. At higher inclination angles ϕ= 30^o (Fig 21c), ϕ=45^o (Fig 21d), and ϕ= 60^o (Fig 21e), natural convection from the lower surface decreased and stable stratification increased with increased inclination angle. Higher Rayleigh promoted natural convection.

Table 2 presents a summary of the numerical investigations on the natural convection induced by the selective absorption of radiation in a fluid layer found in literature.

A systematic comparison of the models developed to date have successfully given insights into the physical processes encountered in induced natural convection in reservoirs. Most of the models have accounted for the depth-dependent absorption of solar radiation within fluid depths using a single value, solar weighted, absorption coefficient and a Total Solar Intensity (TSI) value. The major drawback of applying single bulk values for the absorption coefficient as obtained from an equation is that they are characteristic of the

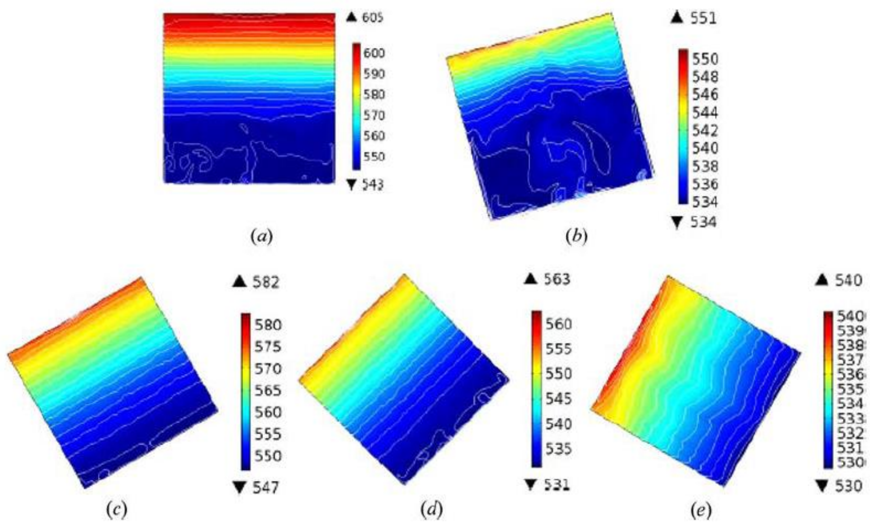

Figure 21: Transient surface temperature plots for ϕ values: (a) 0^o (b) 15^o (c) 30^o (d) 45^o (e) 60^o [48].

visible part of the spectrum, where the salt is mostly transparent to radiation. As such the models fail to account for the effects of the longer wavelengths [24]. Other numerical models have been developed which have accounted for the spectral volumetric absorption of solar radiation in fluid depths, using spectral band models [52, 49]. In spectral band models, an average extinction coefficient k_j and an energy component B_j over each wavelength band are employed to estimate the spectral depth-dependent absorption of solar radiation in fluid layers. Lenert and Wang [50] used a two-band model in a numerical study on "Optimisation of Nano fluid volumetric receivers for solar thermal energy conversion". Webb and Viskanta [51] studied the absorption of solar radiation and heat transfer in a directly-irradiated, thin, falling molten salt film based on two- and three-band attenuation models. Their results showed the sensitivity of their calculations to absorption coefficient band models where the two-band model was found to give higher system performance compared with the three band model [51]. Hattori et al. [52] used a three band attenuation model to study the unsteady natural convection induced by absorption of solar radiation, with relevance to littoral waters. Wu et al. [49], studied the volumetric heat release inside a heat transfer fluid based on a six band attenuation spectral model. The study made comparisons between results of a six-band spectral model with those of a twenty-band solar spectrum model and results were said to be in good agreement [49]. Discrepancies exists between conclusions of the study of Wu et al. [49] and findings of Webb and Viskanta [51]. The latter reports considerable differences between a 2 and 3 band model, which are expected to depend on the resolution of the spectral band. However estimating spectral radiation and wavelength attenuation coefficient of a fluid by bands has been found to lead to errors. Gueymard [53] discusses the drawbacks of the band models with regards to solar intensity distribution and shows the limitations of employing band models over his parametrised models spectra transmittance models. According to Gueymard [53], using a small number of wavelengths in the band model limits the accuracy of the modelled attenuation, particularly in spectral bands where strong absorption exists.

5. Conclusion

A comprehensive review on the on the up to date progress made on radiation induced natural convection in reservoirs primarily heated by absorption of solar radiation has been performed and presented. Results from experimental, numerical and theoretical investigations by comparison are seen to reveal consistent heat transfer and fluid dynamics. Generally, the temperature fields are described as non-linear temperature profile consists of two distinct layers: stable stratified surface layer and a thermal boundary layer are present. Flow development reveals three basic flow stages, an initial a transitional and a quasi steady state stages. The heat transfer mechanisms and flow structures, and development obtained from the various research approaches are consistent and in good agreement. The observed challenges and short comings the respective research approaches for the present problem is addressed as well.

Table 2: Summary of the numerical investigations on the natural convection induced by the selective absorption of radiation in a fluid layer in various enclosures.

Author	Geometry	Method	Remarks
Lei and Patterson [6, 7, 9]	Triangular	Two dimensional Finite volume method. SIMPLE scheme adopted for pressure velocity coupling and QUICK scheme applied for spatial derivatives. Second order implicit scheme used for time discretisation. Three dimensional Finite Difference Method. Discretised using second order differencing and upwind scheme. Second order time accurate backward differencing scheme applied to time integration.	Natural convection and flow development from an isothermal and stationary state in a reservoir side arm subject to solar radiation are shown to occur through an initial stage, transitional stage and quasi steady state.
Hattori et al. [29, 35]	Paralleplied	Finite volume SNS code, Adams-Bashforth and CrankNicolson time discretisation schemes, second-order central differencing, ULTRA (universal limiter for tight resolution and accuracy) flux limiter. The strongly implicit procedure (SIP).	Analytical solution for temperature shows temperature stratification consists of an upper stable stratification and a lower unstable stratification. Nonlinear temperature stratification limitation of the mixing driven by rising thermal plumes, stability, properties of the flow are independent of the Prandtl number and
Hill [32]	Rectangular	compound matrix and Chebyshev-tau techniques.	Linear internal heat source from absorption of radiation based on constants of proportionality.
Harfash [33, 34]	cuboid	velocity-vorticity formulation	Linear theory is very accurate in predicting the onset of convective motion, and thus, regions of stability. Convection has three different patterns.
Webb & Viskanta [39]	Rectangular	Discretised using the control volume scheme of Patankar. SIMPLE algorithm was used to couple pressure and momentum.	Volumetric heat source accounted for based on weighted mean absorption coefficient and constant isotropic solar radiation.
Onyegegbu [40]	Rectangular	Finite difference and implicit method. Internal heat generation based on combined mean Planck, Roseland and scattering coefficients	Convection is found to set in as two counter-rotating eddies of unequal strength. Convection is seen to be encouraged by lowering the optical thickness of the fluid and increasing the albedo. The bottom boundary emissivity is important only at low and intermediate optical thicknesses where lowering boundary emissivity suppresses convection.
Verevochkin and Startsev [41]	Rectangular	Finite volume method with expansion of variables in a Fourier series with time dependent coefficients.	Three different regimes found: intermittent convection, steady-state convection, and free convection. The transitions occur at different values of J0/Q, the ratio of downward solar-radiation flux just below the surface to heat flux through the interface (assumed to be constant), but at almost the same Rayleigh number. The generalized heat-conduction law is found to be valid.
Coates and Patterson [42]	rectangular	Finite Volume method with the SIMPLE scheme, QUICK scheme. Time integration discretised by second order Crank-Nicholson predictor corrector method	Intrusion velocities and transition times determined. Results from code agree with earlier experiments over a range of radiation parameters.

Table 1 (Continued): Summary of the numerical investigations on the natural convection induced by the selective absorption of radiation in a fluid layer in various enclosures.

Author	Geometry	Method	Remarks
Dittko et.al [43]	Tetrahedron domain	Cartesian grid with an Immersed Boundary Method	Significant differences were predicted by the theoretical scaling analysis compared to the triangular domain as presented in the literature. Complex flow patterns were found to be present including helical flow. These features were not accounted for by the theoretical scaling analysis. Despite the complex flow features a number of similar empirical scaling relationships have been found for the tetrahedron cavity based on the numerical results. In particular, the volumetric transfer rate for the cavity was found to vary with the cube root of the Rayleigh number. Relationships were also found for the transition locations between different flow regimes. The original theoretical scaling results were found to provide qualitative information on the locations of different flow regimes and predicted the presence of turbulent flow well. The empirical relationships described have potential applications in large scale lake models. Rather than explicitly resolving sidearms they can be represented by a simple model that uses these relationships as a basis. Further work is needed, however, to better understand the role of the aspect ratios in these models.
Bednarz et.al [44–46]	Triangular	a finite volume method with a double precision solver. A second-order time accurate formulation. Spatial derivatives used a third-order MUSCL scheme conceived by blending a central differencing scheme, second-order upwind scheme, Pressurevelocity and SIMPLE algorithm.	Stable stratification of the water body during the heating phase and an unsteady mixing flow in the reservoir during the cooling phase. Thermal instabilities play an important role in breaking up the residual circulation and initiating a reverse flow circulation in deep waters when the thermal conditions change from heating to cooling. If cooling is sufficiently strong, a clear undercurrent is formed, bringing cold water to the deep region of the reservoir. Heating from the water surface results in a stable large-scale convective roll which is clearly observed in the simulations
Amber & O'Donovan [47, 48]	Square	Finite Element Method with implicit back stepping method. Second-order and linear elements discretisation were applied for the velocity and the pressure field, (P_2+P_1).	Nonlinear temperature profile consisting of distinct layers where thermocapilarity and buoyancy effects are evident. Fluid flow development in the lower layer is found to vary significantly with time and exhibits an initial stage, transitional stage and quasi-steady stages. The magnitude of the natural convection and the duration of each stage is found to decrease as the aspect ratio increases from 0.5 to 2. Calculation of the average heat transfer reveals that the Nusselt Rayleigh number relationship is not uniformly linear and the average heat transfer over the lower boundary surface increased with increasing Ra. Increasing the inclination angles decreases the natural convection and increases stratification. Higher Rayleigh number promotes natural convection.

References

[1] Monismith, S.G. and J. Imberger, J. and Morison, M.L. *Convective motions in the sidearm of a small reservoir* Limnol. Oceanogr. 35 pp.16761702 1990.

[2] Adams, E.E. and Wells, S.A. *Field measurements on side arms of lake.* Anna, VA, J.Hydraul. 110 pp 773793 1984.

[3] Kirk, J.T.O. *Optical limnology a manifesto* Limnol. Aust, Springer, Netherlands, pp. 3362, 1986.

[4] Dugaria, S. and Bortolato, M. and Del Col, D. *Modelling of a direct absorption solar receiver using carbon based nanofluids under concentrated solar radiation.* Renewable Energy, 113: 444–455, 2017.

[5] Farrow,D.E. and Patterson, J.C. *On the stability of the near shore waters of a lake when subject to solar heating.* Int. J. Heat Mass Transf. 36, 89100, 1993

[6] Lei,C. and Patterson, J. C. *Natural convection in a reservoir sidearm subject to solar radiation: experimental observations.* Experiments in Fluids;32(5):590-599, 2002.

[7] Lei,C. and Patterson,J. C. *Natural convection in a reservoir sidearm subject to solar radiation: A two-dimensional simulation.* Numerical Heat Transfer: Part A: Applications;42(1-2):13-32, 2002

[8] Lei,C. and Patterson,J. C. *A direct three-dimensional simulation of radiation-induced natural convection in a shallow wedge.* International Journal of Heat and Mass Transfer;46(7):1183-1197, 2003

[9] Lei,C. and Patterson,J. C. *A direct stability analysis of a radiation-induced natural convection boundary layer in a shallow wedge.* Journal of Fluid Mechanics;480:161-184, 2003

[10] Mao, Y. and Lei,C. and Patterson,J. C. *Unsteady natural convection in a triangular enclosure induced by absorption of radiation: a revisit by improved scaling analysis.* Journal of Fluid Mechanics;622(5):75-102, 2009.

[11] Tetreault-Friend, M. and Gray, L. A. and Berdibek, S. and McKrell, T. and Slocum, A. H. *Optical properties of high temperature molten salt mixtures for volumetrically absorbing solar thermal receiver applications.* Solar Energy, 153: 238–248, 2017.

[12] Tahereh B. Gorji and A.A. Ranjbar *A review on optical properties and application of nanofluids in direct absorption solar collectors (DASCs).* Renewable and Sustainable Energy Review, 72: 10–32, 2017.

[13] Walden, R. W., and Guenter Ahlers. *Non-Boussinesq and penetrative convection in a cylindrical cell.* Journal of Fluid Mechanics 109 89-114, 1981.

[14] Behringer, R. P. and Ahlers, G. *Heat transport and temporal evolution of fluid flow near the Rayleigh-Bénard instability in cylindrical containers.* Journal of Fluid Mechanics 125 219–258, 1982.

[15] Webb, B.W. and Viskanta, R. *Radiation-induced buoyancy-driven flow in rectangular enclosures: experiment and analysis.* American Society of Mechanical Engineers, Journal of Heat Transfer, 109(2):427-433, 1988.

[16] Coates, M. J. and Patterson, J. C. *Unsteady natural convection in a cavity with non-uniform absorption of radiation.* Journal of Fluid Mechanics:133-161, 1993

[17] Krishnamurti, R. *Convection induced by selective absorption of radiation: A laboratory model of conditional instability.* Dynamics of Atmospheres and Oceans, 27, 14, 367-382, 1998.

[18] Lei,C. and Patterson,J. C. *Unsteady natural convection in a triangular enclosure induced by absorption of radiation.* Journal of Fluid Mechanics;460(4):181-209, 2002.

[19] Moroni, M., and A. Cenedese. *Penetrative convection in stratified fluids: velocity and temperature measurements.* Nonlinear processes in Geophysics 13, 3 353-363, 2006.

[20] Dore. V Moroni, M. Menach , M. Cenedese A. *Investigation of penetrative convection in stratified fluids through 3D-PTV* Exp Fluids 47:811825 2009

[21] Bednarz, T.P. and Lei, C. W. and Patterson, J.C. *An experimental study of unsteady natural convection in a reservoir model cooled from the water surface*. Exp. Therm. Fluids 32, 844856 2009.

[22] Naghib, A. and Hattori, T. Patterson, J.C., Lei, C. *Natural convection induced by radiation in a water filled square cavity: Experimental observations*. Experimental Thermal and Fluid Science 80 105116, 2017.

[23] Viskanta R and Toor J. S. *Absorption of solar radiation in ponds.* Solar Energy, 21(1):17-25, 1978.

[24] Cengel Y. A. and Ozisik M. N. *Solar radiation absorption in solar ponds.* Solar Energy, 33(6):581-591, 1984.

[25] Estoque M.A. *Vertical mixing due to penetrative convection.* Journal of the Atmospheric Sciences: 1046-1051, 1968

[26] Farrow D.E. and Patterson, J.C. *On the response of a reservoir sidearm to diurnal heating and cooling* . J.Fluid Mech. 246, 143-161, 1993

[27] Cormack, D.E. and Leal, L.G and Imberger, J. *Natural convection in a shallow cavity with differentially heated end walls. Part 1. Asymptotic theory.* J.Fluid Mech. 65, 209-229, 1973

[28] Farrow D.E. and Patterson, J.C. *The daytime circulation and temperature structure in a reservoir sidearm.* Int. J. Heat Mass Transf. 37, 19571968, 1994

[29] Hattori, T. and Patterson, J.C. and Lei, C. *Mixing in internally heated natural convection flow and scaling for a quasi-steady boundary layer.* Journal of Fluid Mechanics:763 352-368, 2015

[30] Mao, Y., Lei,C. and Patterson, J. C. *Characteristics of instability of radiation-induced natural convection in shallow littoral waters*. International Journal of Thermal Sciences:49(1)170–181, 2010

[31] Mao, Y., Lei,C. and Patterson, J. C. *Unsteady near shore natural convection induced by surface cooling*. Journal of Fluid Mechanics:642 213–233, 2010

[32] Hill, A. A. *Penetrative convection induced by the absorption of radiation with a nonlinear internal heat source.* Dynamics of Atmospheres and Oceans 38, 1, 5767, 2004.

[33] Harfash, A. J. *Three-dimensional simulations and stability analysis for convection induced by absorption of radiation*. International Journal of Numerical Methods for Heat & Fluid Flow:25(4) 810–824, 2015

[34] Harfash, A. J. *Three-dimensional simulations and stability analysis for convection induced by absorption of radiation*. International Journal of Numerical Methods for Heat & Fluid Flow:25(4) 810–824, 2015

[35] Hattori, T. and Patterson, J.C. and Lei, C. *Scaling and direct stability analyses of natural convection induced by absorption of solar radiation in a parallelepiped cavity*. International Journal of Thermal Sciences:88 19-32, 2015

[36] Hattori, T. and Patterson, J.C. and Lei, C. *On the stability of internally heated natural convection due to absorption of radiation in a laterally confined fluid layer with a horizontal through flow*. International Journal of Heat and Mass Transfer:81 846-861, 2015

[37] Hattori, T. and Patterson, J.C. and Lei, C. *Characterisation of linear and oscillatory behaviours of radiation induced natural convection boundary layer in response to constnt and time varying thermal forcing* . International Journal of Heat and Mass Transfer:87 24-35, 2015

[38] Hattori, T. and Patterson, J.C. and Lei, C. *On the stability of transient penetrative convection driven by internal heating coupled with a thermal boundary condition.* International Communication in Heat and Mass Transfer:64 29-33, 2015

[39] Webb, B.W. and Viskanta, R. *Analysis of radiation-induced natural convection in rectangular enclosures*. Journal of Thermophysics and Heat Transfer, vol. 1:146-153, 1987

[40] Onyegegbu S. *Solar-radiation induced natural-convection in stagnant water layers*. Energy Conversion and Management; 30:91-100, 1990.

[41] Verevochkin Y.G., Startsev S.A. *Numerical Simulation of Convection and Heat Transfer in Water Absorbing Solar Radiation.* Journal of Fluid Mechanics ;421:293-305, 2000.

[42] Coates, M. J. and Patterson, J. C. *Numerical simulations of the natural convection in a cavity with nonuniform internal sources.* International journal of heat and fluid flow; 15,(3):218–225, 1994

[43] Dittko, K.A. and Kirkpatrick, M.P and Armfield, S.W. *Numerical simulations turbulent natural convection in a shallow tetrahedron domain* Physics of Fluids 25, 025105 1-26

[44] Bednarz, T.P. and Lei, C and Patterson, J.C. *Unsteady natural convection induced by diurnal temperature changes in a reservoir with slowly varying bottom topography.* International Journal of Thermal Sciences:48 19321942, 2009

[45] Bednarz, T.P. and Lei, C. W. and Patterson, J.C. *An experimental study of unsteady natural convection in a reservoir model subject to periodic thermal forcing using combined PIV and PIT techniques.* Exp. Fluids 47, 107117 2009.

[46] Bednarz, T.P. and Lei, C and Patterson, J.C. *A numerical study of unsteady natural convection induced by iso-flux surface.* International Journal of Heat Mass Transfer 52 5666, 2009

[47] Amber I. and ODonovan T. S. *Heat transfer in a molten salt filled enclosure absorbing concentrated solar radiation.* International Journal of Heat and Mass Transfer, 113: 444–455, 2017.

[48] Amber I. and ODonovan T. S. *numerical simulation of heat transfer in an enclosure with a nonlinear heat source.* Numerical Heat Transfer, Part A: Applications, 71(11): 1081–1093, 2017.

[49] Hongbo W., Runsheng T., Zhimin L, and Hao Z. *A mathematical procedure to estimate solar absorptance of shallow water ponds.* Energy Conversion and Management, 50(7): 1828-1833, 2009.

[50] Lenert A and Wang E. N. *Optimization of nanofluid volumetric receivers for solar thermal energy conversion.* Solar Energy, 86(1):253-265, 2012.

[51] Webb B. W. and Viskanta R. *Analysis of heat transfer and solar radiation absorption in an irradiated thin, falling molten salt film.* Journal of solar energy engineering, 107(2): 113-119, 1985.

[52] Hattori T. Patterson J. C. and C Lei C. *Study of unsteady natural convection induced by absorption of radiation based on a three-waveband attenuation model.* Journal of Physics: Conference Series, volume 530, page 012036.

[53] Gueymard C. A., Myers D, and Emery K. *Proposed reference irradiance spectra for solar energy systems testing.* Solar energy, 73(6): 443-467, 2002.